

Elastic strain engineering of ferroic oxides

Darrell G. Schlom, Long-Qing Chen, Craig J. Fennie, Venkatraman Gopalan, David A. Muller, Xiaoqing Pan, Ramamoorthy Ramesh, and Reinhard Uecker

Using epitaxy and the misfit strain imposed by an underlying substrate, it is possible to elastically strain oxide thin films to percent levels—far beyond where they would crack in bulk. Under such strains, the properties of oxides can be dramatically altered. In this article, we review the use of elastic strain to enhance ferroics, materials containing domains that can be moved through the application of an electric field (ferroelectric), a magnetic field (ferromagnetic), or stress (ferroelastic). We describe examples of transmuting oxides that are neither ferroelectric nor ferromagnetic in their unstrained state into ferroelectrics, ferromagnets, or materials that are both at the same time (multiferroics). Elastic strain can also be used to enhance the properties of known ferroic oxides or to create new tunable microwave dielectrics with performance that rivals that of existing materials. Results show that for thin films of ferroic oxides, elastic strain is a viable alternative to the traditional method of chemical substitution to lower the energy of a desired ground state relative to that of competing ground states to create materials with superior properties.

The strain game

For at least 400 years, humans have studied the effects of pressure (hydrostatic strain) on the properties of materials.[1] In the 1950s, it was shown that biaxial strain, where a film is clamped to a substrate but free in the out-of-plane direction, can alter the transition temperatures of superconductors[2] (T_c) and ferroelectrics (T_C).[3]

What has changed in recent years is the magnitude of the biaxial strain that can be imparted. Bulk ferroic oxides are brittle and will crack under moderate strains, typically 0.1%. One way around this limitation is the approach of bulk crystal chemists, to apply "chemical pressure" through isovalent cation substitution. A disadvantage of such a bulk approach, however, is the introduction of disorder and potentially unwanted local distortions. Epitaxial strain, the trick of the thin-film alchemist, provides a potentially disorder-free route to large biaxial strain and has been used to greatly enhance the mobility of transistors[4,5] (see the article by Bedell et al. in this issue), increase catalytic activity (see the article by Yildiz in this issue), alter band structure[6] (see the article by Yu et al. in this issue), and significantly increase superconducting,[7,8] ferromagnetic,[9–11] and ferroelectric[12–16] transition temperatures. This approach, which we refer to as the "strain game," is illustrated in **Figure 1** for elastically strained films of oxides with the perovskite structure.

Strains of about ±3% are common in epitaxial oxide films today,[17–20] with the record to date being a whopping 6.6% compressive strain achieved in thin $BiFeO_3$ films grown on (110) $YAlO_3$.[21–24] These strains are an order of magnitude higher than where these materials would crack in bulk.[25–27]

Strained $SrTiO_3$ and the importance of suitable substrates

The strain game for ferroics was ignited by the demonstration that an oxide that normally is not ferroelectric at any temperature can be made ferroelectric at room temperature through the application of biaxial strain.[12] Such a gigantic shift in properties and T_C had never before been clearly seen in any

Darrell G. Schlom, Department of Materials Science and Engineering, Cornell University and Kavli Institute at Cornell for Nanoscale Science; schlom@cornell.edu
Long-Qing Chen, Millennium Science Complex, Materials Research Institute, Penn State University; lqc3@psu.edu
Craig J. Fennie, School of Applied and Engineering Physics, Cornell University; fennie@cornell.edu
Venkatraman Gopalan, Materials Science and Engineering, Penn State University; vgopalan@psu.edu
David A. Muller, School of Applied and Engineering Physics, Cornell University and Kavli Institute at Cornell for Nanoscale Science, Cornell; dm24@cornell.edu
Xiaoqing Pan, Department of Materials Science and Engineering, University of Michigan; panx@umich.edu
Ramamoorthy Ramesh, Oak Ridge National Laboratory; rameshr@ornl.gov
Reinhard Uecker, Leibniz Institute for Crystal Growth, Berlin; reinhard.uecker@ikz-berlin.de
DOI: 10.1557/mrs.2014.1

© 2014 Materials Research Society
https://doi.org/10.1557/mrs.2014.1 Published online by Cambridge University Press

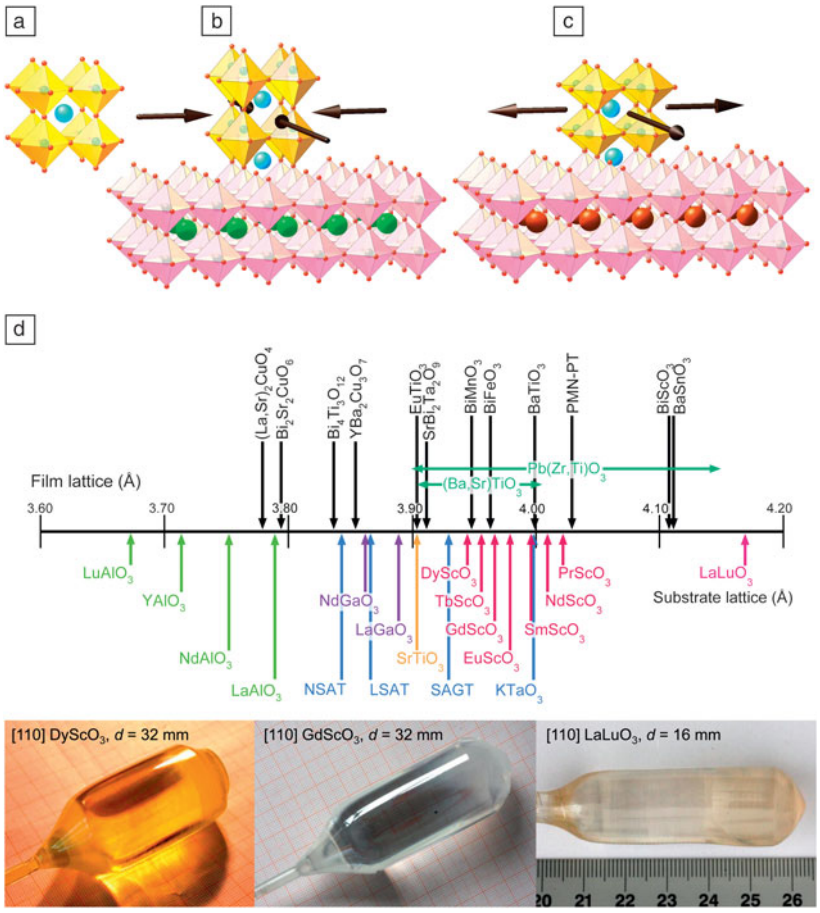


Figure 1. How the "strain game" is used to impart biaxial elastic strain on an oxide film via epitaxy. (a) The crystal structure of an unstrained oxide, in this case an oxide with the perovskite structure, in its unstrained state. When deposited on a substrate with a larger or smaller spacing, the energetic preference of the deposited atoms to follow the template of the underlying substrate (epitaxy) can result in the film beginning in either (b) biaxial compression or (c) biaxial tension. (d) A number line showing the pseudotetragonal or pseudocubic *a*-axis lattice constants in angstroms of some perovskites and perovskite-related phases of interest, including ferroics (above the number line) and of some of the perovskite substrates that are available commercially (below the number line). LSAT, $(LaAlO_3)_{0.29}$—$(SrAl_{1/2}Ta_{1/2}O_3)_{0.71}$; NSAT, $(NdAlO_3)_{0.39}$—$(SrAl_{1/2}Ta_{1/2}O_3)_{0.61}$; SAGT, $Sr_{1.04}Al_{0.12}Ga_{0.35}Ta_{0.50}O_3$. Photographs of exemplary single crystals used as substrates, each with diameter, *d*. (d) An updated version of the plot in Reference 24.

ferroic system; nonetheless, this achievement was the experimental realization of what had been predicted years earlier by theory.[28,29] **Figure 2** shows the strain phase diagram of $(001)_p$ $SrTiO_3$ calculated by thermodynamic analysis,[12,14,15,28–30] where the p subscript indicates pseudocubic Miller indices. These predictions imply that a biaxial tensile strain on the order of 1% will shift the T_C of $SrTiO_3$ to the vicinity of room temperature.[12,28–32] Although many researchers had grown $SrTiO_3$ films on substrates with different spacings, the lattice mismatches were so large and the films so thick that the films were no longer elastically strained.

Fully commensurate, elastically strained epitaxial films have the advantage that high densities of threading dislocations (e.g., the ~10^{11} dislocations cm^{-2} observed, for example, in partially relaxed $(Ba_xSr_{1-x})TiO_3$ films)[33,34] are avoided. Strain fields around dislocations locally alter the properties of a film, making its ferroelectric properties inhomogeneous and often degraded.[35–37] To achieve highly strained ferroic films and keep them free of such threading dislocations, one needs to keep them thin, typically not more than a factor of five beyond the Matthews-Blakeslee critical thickness, beyond which it becomes energetically favorable (though typically constrained by kinetics) for a film to relax by the introduction of dislocations.[27,38] Thickness-dependent studies, involving the growth of a ferroic on just one substrate material to study the effect of strain in partially relaxed films, are not as easy to interpret as experiments utilizing commensurate films grown on several different substrate materials covering a range of lattice spacings. In the former, the strains are inhomogeneous, and the high concentration of threading dislocations can obfuscate intrinsic strain effects.

Exploring the strain predictions in Figure 2a was greatly simplified by the development of new substrates with a broad range of spacings to impart a desired strain state into the overlying $SrTiO_3$ film. These substrates have the same structure as $SrTiO_3$—the perovskite structure—but different lattice spacings. The number of perovskite single crystals that are available commercially as large substrates (with surfaces at least 10 mm × 10 mm in size) has nearly doubled in the last decade due to the work of the present authors.[39–41] Today, various single crystal perovskite and perovskite-related substrates are commercially available (see Figure 1d), including $LuAlO_3$,[42,43] $YAlO_3$,[44] $LaSrAlO_4$,[45] $NdAlO_3$,[46] $LaAlO_3$,[47,48] $LaSrGaO_4$,[49] $(NdAlO_3)_{0.39}$—$(SrAl_{1/2}Ta_{1/2}O_3)_{0.61}$ (NSAT),[50] $NdGaO_3$,[51,52] $(LaAlO_3)_{0.29}$—$(SrAl_{1/2}Ta_{1/2}O_3)_{0.71}$ (LSAT),[50,53] $LaGaO_3$,[54] $SrTiO_3$,[55–58] $Sr_{1.04}Al_{0.12}Ga_{0.35}Ta_{0.50}O_3$ (SAGT), $DyScO_3$,[12,39] $TbScO_3$,[40] $GdScO_3$,[13,39,59] $EuScO_3$, $SmScO_3$,[39,60] $KTaO_3$,[61] $NdScO_3$,[39,62] $PrScO_3$,[63] and $LaLuO_3$;[64] many of these are produced with structural perfection rivaling that of conventional semiconductors. The perfection of the substrate, the best of which are grown by the Czochralski method (which is not applicable to most ferroic oxides because they do not melt congruently), can be passed on to the film via epitaxy. This has led to the growth of strained epitaxial films of the ferroics $SrTiO_3$,[38,65] $BaTiO_3$,[14] $BiFeO_3$,[66] $BiMnO_3$,[67] and $EuTiO_3$,[16] with rocking curve full width at half maximum values ≤11 arcsec (0.003°)—identical to those of the commercial substrates upon which they are grown and significantly narrower

https://doi.org/10.1557/mrs.2014.1 Published online by Cambridge University Press

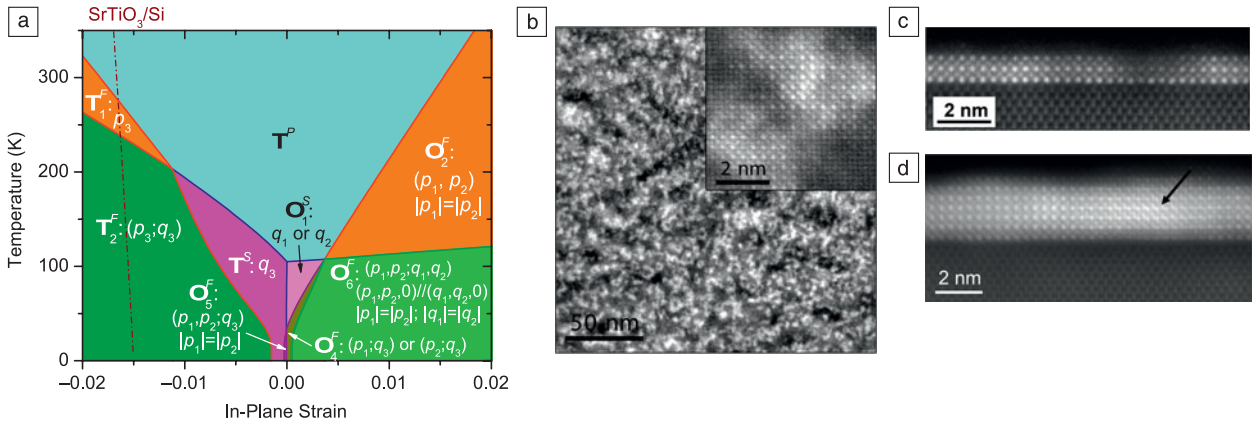


Figure 2. (a) The strain phase diagram of $(001)_p$-oriented $SrTiO_3$ calculated assuming a single-domain state for all structural and ferroelectric phases. The letters T and O used in the phase notations indicate tetragonal and orthorhombic crystallographic symmetries, respectively, under a constraint. The paraelectric, ferroelectric, and ferroelastic (or antiferrodistortive structural) natures of the phases are revealed by the superscripts *P*, *F*, and *S*, respectively. The components of the polarization vector **P** corresponding to the phases (along the crystallographic directions of pseudocubic $SrTiO_3$) are indicated within the parentheses following the phase notation. The dashed line corresponds to $(001)_p$ $SrTiO_3$ commensurately strained to (001) Si. At room temperature, it is strained in biaxial compression by ~1.7%. This strain decreases slightly with temperature due to the larger thermal expansion coefficient of $SrTiO_3$ than silicon. (b) Plan-view and (c) cross-sectional annular dark field (ADF) scanning transmission electron microscopy (STEM) images of a nominally 2 unit-cell-thick (0.8 nm) epitaxial $(001)_p$ $SrTiO_3$ film grown on (001) Si and capped with amorphous silicon. (d) Cross-sectional ADF-STEM images of a nominally 5 unit-cell-thick (2.0 nm) commensurate epitaxial $(001)_p$ $SrTiO_3$ film grown on (001) Si. The image shows an average film thickness of 6.5 unit cells, suggesting nonuniform $SrTiO_3$ coverage. In the area marked with an arrow, more than one $SrTiO_3$ grain is imaged in projection. (a) Adapted from References 14 and 15 and has only a minor difference from that presented in References 28 and 29. (b) and (c) Reprinted with permission from Reference 78. © 2008 American Physical Society. (d) Reprinted with permission from Reference 15. © 2009 AAAS.

(indicative of higher structural perfection) than the most perfect bulk single crystals of these same materials.

Using these new perovskite substrates, predictions of the $SrTiO_3$ strain phase diagram shown in Figure 2 were assessed. Not only was it found possible to transmute $SrTiO_3$ into a room temperature ferroic,[12,68,69] but the experimentally determined point group,[31,32,70–72] direction and magnitude of spontaneous polarization (P_S),[31,32,65,70–73] observed shifts in T_C [12,70,71] and soft mode frequency with biaxial strain,[74] and existence of a transition to a simultaneously ferroelectric and ferroelastic phase at lower temperatures[70–72,74] were all in accord with theory. Not all of the experimental observations, however, were in agreement with theory. For example, it was observed that strained $SrTiO_3$ films exhibit a significant frequency dependence to their dielectric response.[65,73] This relaxor ferroelectric behavior is due to defects. On account of the strain, the $SrTiO_3$ matrix is highly polarizable and can be easily polarized by defect dipoles that arise from non-stoichiometry in the $SrTiO_3$ film. Based on how the properties of strained $SrTiO_3$ films vary with non-stoichiometry, strained, perfectly stoichiometric $SrTiO_3$ films are not expected to show relaxor behavior.[75]

To make it possible for strain-enabled or strain-enhanced functionalities to be exploited in mainstream device architectures, it is desirable to play the strain game on substrates relevant to the semiconductor industry. One such example is the integration of commensurately strained $SrTiO_3$ films with silicon.[15] The lattice mismatch between $(001)_p$ $SrTiO_3$ and (001) Si is 1.7%, as indicated by the dashed line on the left side of the strain phase diagram in Figure 2a. From theory (Figure 2a), such a film would be expected to be ferroelectric with a T_C near room temperature. This integration is, however, rather challenging due to (1) the high reactivity of silicon with many elements and their oxides,[76,77] and (2) the thermodynamic driving force for a pristine silicon surface to oxidize and form an amorphous native oxide (SiO_2), which blocks epitaxy, under the oxidizing conditions typically used for the growth of oxide thin films. Despite these impediments, thin commensurate $SrTiO_3$ films have been grown directly on silicon without discernible intermediate layers and free of reaction, and are found to be ferroelectric at room temperature.[15]

Planar-view and cross-sectional annular dark field (ADF) scanning transmission electron micrographs (STEM) of epitaxial $(001)_p$ $SrTiO_3$ films grown on and commensurately strained to (001) Si are shown in Figure 2b–d. Although the interface between $SrTiO_3$ and silicon is seen to be abrupt and free of reaction, these images reveal additional challenges to the growth of $SrTiO_3$ on silicon. First is the propensity of $SrTiO_3$ to nucleate as islands and not wet the surface of the silicon substrate.[78] Even using kinetically limited growth conditions,[15,79] it takes multiple unit cells of growth before the $SrTiO_3$ islands coalesce.[78] Second are frequent out-of-phase boundaries in the $SrTiO_3$ film (see Figure 2d) resulting from the step height of (001) Si (0.14 nm) not matching the step height of $(001)_p$ $SrTiO_3$ (0.39 nm). Out-of-phase boundaries can form during the coalescence of $SrTiO_3$ islands that have nucleated on different (001) Si terraces. The arrow in Figure 2d marks an area where the $SrTiO_3$ islands are out-of-phase with each other.

https://doi.org/10.1557/mrs.2014.1 Published online by Cambridge University Press

For the growth of high-quality films of ferroic oxides with a desired strain state, not only are appropriate substrates of exceptionally high perfection needed, but also methods to prepare them with smooth, well-ordered surfaces with a specific chemical termination on which epitaxial growth can be reliably initiated. For example, chemical-mechanically polished (001) $SrTiO_3$ substrates display a mixture of SrO- and TiO_2-terminated surfaces. A combination of chemical etching and annealing has been shown to yield $SrTiO_3$ substrates with known surface termination. Kawasaki et a1.[80] showed that an NH_4F-buffered HF solution with controlled pH enables etching of the more basic SrO layer and leaves a completely TiO_2 terminated surface on the substrate. This method of preparing a TiO_2-terminated (001) $SrTiO_3$ surface has been further perfected by Koster et a1.[81] SrO-terminated (001) $SrTiO_3$ substrates can also be prepared.[82] A means to prepare low defect surfaces with controlled termination has since been developed for (110) $SrTiO_3$,[83] (111) $SrTiO_3$,[83,84] $(001)_p$ $LaAlO_3$,[85,86] $(111)_p$ $LaAlO_3$,[85] (110) $NdGaO_3$,[86] $(001)_p$ LSAT,[86,87] (110) $DyScO_3$,[88,89] (110) $TbScO_3$,[88] (110) $GdScO_3$,[88] (110) $EuScO_3$,[88] (110) $SmScO_3$,[88] (001) $KTaO_3$,[90] (110) $NdScO_3$,[88] and (110) $PrScO_3$[88] substrates.

The strain game is capable of enhancing the properties of a multitude of ferroelectric systems. Shifts in ferroelectric T_C of roughly 300 K per percent biaxial strain, quite comparable to those predicted[28–32] and observed[12,68–74] for $SrTiO_3$, were first predicted by theory and subsequently verified by experiments on biaxially strained $BaTiO_3$[13,14,91–94] and $PbTiO_3$[14,91,95–100] films. Strain effects of comparable magnitude have also been observed in strained (Ba,Sr)TiO_3 films[101,102] and in strained-layer superlattices: $KTaO_3/KNbO_3$,[103] $SrTiO_3/SrZrO_3$,[104] $SrTiO_3/BaZrO_3$,[105] $PbTiO_3/SrTiO_3$,[106,107] $BaTiO_3/SrTiO_3$,[108–111] and $CaTiO_3/SrTiO_3/BaTiO_3$.[112–114]

The success of theory in predicting the effect of strain on a multitude of ferroelectrics, together with advances in the ability to customize the structure and strain of oxide heterostructures at the atomic-layer level, has enabled a new era: ferroelectric oxides by design.[14] The appropriate theoretical methods to design strain-enhanced ferroelectrics depend on the material and whether or not domains need to be taken into account. First-principles methods are good for new materials where the coefficients of the Landau–Devonshire free energy expansion,[30] a Taylor expansion of the free energy of a material in powers of its order parameter (polarization for typical ferroelectrics), are unknown. Due to the relatively small number of atoms that can be included in such calculations, however, the calculations are limited to single-domain materials. Measurements on materials can yield the coefficients needed in Landau–Devonshire thermodynamic analysis to calculate the effect of strain in the absence of domains.[30]

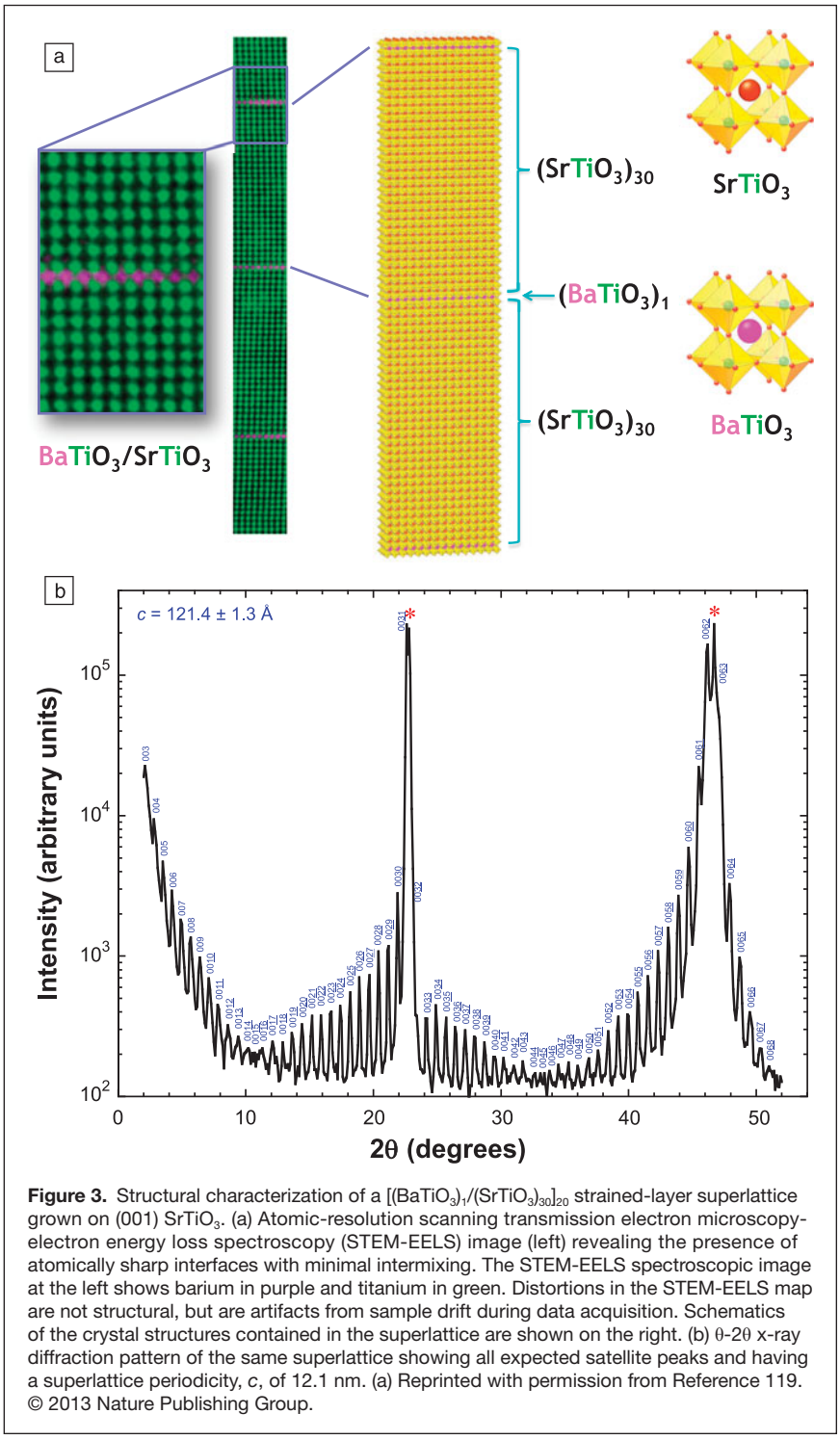


Figure 3. Structural characterization of a $[(BaTiO_3)_1/(SrTiO_3)_{30}]_{20}$ strained-layer superlattice grown on (001) $SrTiO_3$. (a) Atomic-resolution scanning transmission electron microscopy-electron energy loss spectroscopy (STEM-EELS) image (left) revealing the presence of atomically sharp interfaces with minimal intermixing. The STEM-EELS spectroscopic image at the left shows barium in purple and titanium in green. Distortions in the STEM-EELS map are not structural, but are artifacts from sample drift during data acquisition. Schematics of the crystal structures contained in the superlattice are shown on the right. (b) θ-2θ x-ray diffraction pattern of the same superlattice showing all expected satellite peaks and having a superlattice periodicity, *c*, of 12.1 nm. (a) Reprinted with permission from Reference 119. © 2013 Nature Publishing Group.

https://doi.org/10.1557/mrs.2014.1 Published online by Cambridge University Press

Phase-field simulations, which also require coefficients obtained from either experiment or first-principles calculations, can be used to take domains into account.[97,98] An example is $(BaTiO_3)_n/(SrTiO_3)_m$ strained-layer superlattices, where n and m refer to the thickness, in unit cells, of the $(001)_p$ $BaTiO_3$ and $(001)_p$ $SrTiO_3$ layers, respectively. Despite the 2.3% lattice mismatch between the $(001)_p$ $BaTiO_3$ and $(001)_p$ $SrTiO_3$ layers, such superlattices can be commensurately strained. In **Figure 3**, the structural characterization of a commensurate $(BaTiO_3)_n/(SrTiO_3)_m$ superlattice with $n = 1$ and $m = 30$ is shown. The macroscopic regularity of this superlattice, which was grown by molecular beam epitaxy (MBE), is demonstrated by the presence and sharpness of all of the superlattice reflections in its x-ray diffraction pattern (see Figure 3b).[60,119] Despite the $BaTiO_3$ layer being just a single unit cell thick (0.4 nm) and well-separated from neighboring $BaTiO_3$ layers, ultraviolet Raman measurements show that it is still ferroelectric.[60]

The ability to compare theory and experiment has motivated refinements in theory, including attention to not only mechanical (strain) and electrical boundary conditions (whether the ferroelectric is bounded by conducting electrodes or insulating layers), but also to unequal biaxial strain[115,116] and the ability of a ferroelectric film to break up into multiple domains.[97,98] For strained-layer superlattices of $BaTiO_3/SrTiO_3$, it was shown that quantitative agreement between the predicted and observed T_C for superlattices with a wide range of periodicities only occurred if calculations in which the possibility of multiple domains was considered.[109,110] For some $BaTiO_3/SrTiO_3$ superlattices, such three-dimensional phase-field calculations indicated that the low energy configuration was a multiple-domain state, which allowed the polarization in the $(001)_p$ $SrTiO_3$ layers to drop considerably when the $(001)_p$ $BaTiO_3$ layer was thinner than the $(001)_p$ $SrTiO_3$ layer, resulting in a significant increase in T_C compared to the single-domain state.[109,110] The domains anticipated to be present by theory, in order to quantitatively explain the observed T_C values, have recently been observed in $BaTiO_3/SrTiO_3$ strained-layer superlattices.[117,118]

Strain engineering of multiferroics

Emboldened by these successes, the strain game has more recently turned to enhancing materials containing multiple ferroic order parameters (i.e., multiferroics such as $BiFeO_3$) or to create new multiferroics from materials that are on the verge of being ferroic (e.g., $EuTiO_3$). Illustrative examples are described in the sections that follow.

Strained $BiFeO_3$—Morphing a room-temperature multiferroic

Bismuth ferrite, $BiFeO_3$, is one of the few materials that is simultaneously ferroelectric and magnetically ordered (antiferromagnetically in the case of $BiFeO_3$) at room temperature.[120–124] All of the other room-temperature multiferroics are, however, metastable. These include the high-pressure phase $BiCoO_3$,[122] strain-stabilized $ScFeO_3$ with the corundum structure,[123] and the hexagonal polymorph of $LuFeO_3$ that has been stabilized via epitaxy.[124] In its unstrained state, $BiFeO_3$ has the highest remnant polarization of any known ferroelectric.[120,121,125–127] $BiFeO_3$ also exhibits several polymorphs that are relatively close in energy to each other. Further, in $BiFeO_3$, the four fundamental degrees of freedom—electronic

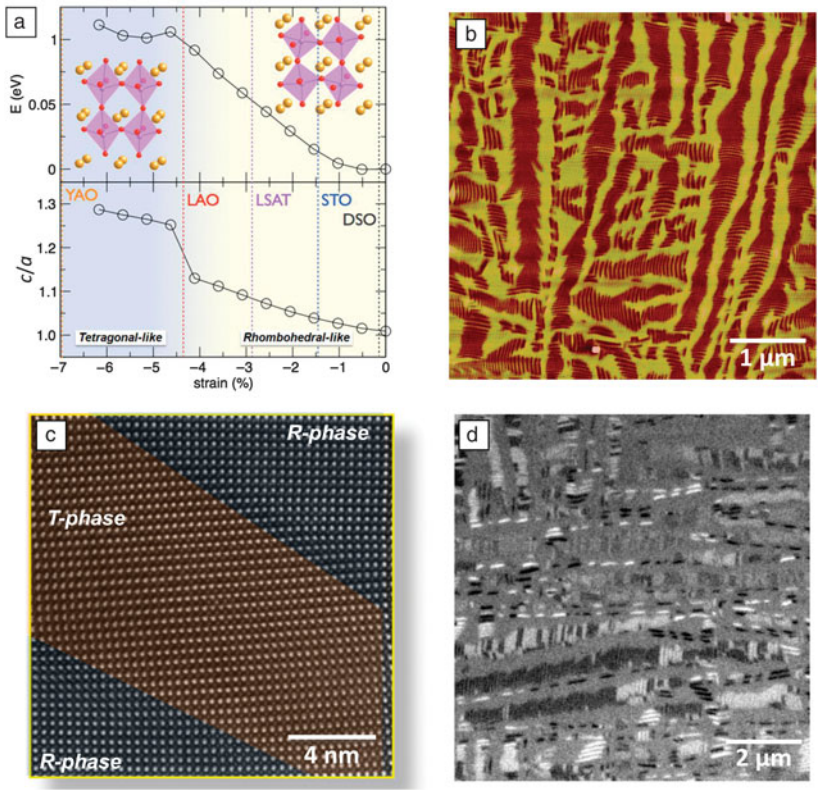


Figure 4. (a) *Ab initio* calculations of the energy and structure (ratio of pseudotetragonal lattice constants *c*/*a*) of the ground state of $BiFeO_3$ as a function of bi-axial, in-plane compressive strain on various substrates: YAO, $YAlO_3$; LAO, $LaAlO_3$; STO, $SrTiO_3$; LSAT, $(LaAlO_3)_{0.29}—(SrAl_{1/2}Ta_{1/2}O_3)_{0.71}$; DSO, $DyScO_3$. (b) Atomic force microscopy image of a partially relaxed, ~70-nm-thick $BiFeO_3$ film grown on a $LaAlO_3$ substrate that exhibits a characteristic tetragonal and rhombohedral (T+R) mixed phase nanostructure. (c) High-resolution transmission electron microscopy image of the T+R mixed phase that illustrates the commensurate nature of the interface, with the complete absence of misfit dislocations. (d) X-ray magnetic circular dichroism photoemission electron microscopy (XMCD-PEEM) image obtained using the iron absorption edge showing that the highly constrained R-phase shows enhanced ferromagnetism compared to the bulk or the T-phase. Enhanced magnetic contrast is given from the ratio of PEEM images taken with left and right circularly polarized x-rays at the same location. Black and white contrasts indicate magnetic moments pointing parallel and antiparallel to the incident x-rays. (a) Reprinted with permission from Reference 21. © 2009 AAAS. (b) Adapted from Reference 21. (c) Reprinted with permission from Reference 21. © 2009 AAAS. (d) Reprinted with permission from Reference 134. © 2011 Nature Publishing Group.

https://doi.org/10.1557/mrs.2014.1 Published online by Cambridge University Press

spin, charge, orbital, and lattice—are highly interactive. As a consequence, its ground state exhibits a strong sensitivity to temperature, pressure, electric fields, and magnetic fields. These qualities make $BiFeO_3$ unique and a natural candidate to tweak using the strain game.

Elastic strain, imparted via epitaxy, is able to distort and eventually change the structure and energy of the ground state of $BiFeO_3$. In its unstrained state, $BiFeO_3$ is rhombohedral.[128] The evolution of the structure of $BiFeO_3$ can be understood from *ab initio* calculations, **Figure 4**a. As an in-plane biaxial compressive strain is imposed via the substrate, the rhombohedral (R) structure becomes progressively monoclinic (and perhaps even triclinic) until a critical strain of ~4.5% is reached. For substrates that impose a larger strain (such as (110) $YAlO_3$, which imposes a hefty 6.6% biaxial compressive strain on commensurate $BiFeO_3$ thin films grown upon it[21–24]), the structure changes into a "super-tetragonal" (T) state (or a monoclinic derivative thereof) with a distinct jump in the ratio of its pseudotetragonal lattice constants c/a.[21] Such an isostructural monoclinic-to-monoclinic phase transition—in which the symmetry does not change, but the coordination chemistry changes dramatically—has also been observed in other materials.[129–132] The overlapping, roughly parabolic free energy versus strain curves of the R- and T-phases can be seen in Figure 4a. It is the change in ground state with strain from the R phase to the T phase that enables the huge (6.6%) biaxial strains to be achieved in $BiFeO_3$ films. In more typical oxide systems, the free energy versus strain landscape limits the growth of epitaxial perovskite films under common growth conditions to about 3% strain.

Partial relaxation of the epitaxial constraint by increasing the film thickness leads to the formation of a mixed-phase nanostructure that exhibits the coexistence of both the R- and T-phases, as illustrated in the atomic force microscope (AFM) image in Figure 4b. This mixed-phase nanostructure is fascinating from many perspectives. First, high-resolution electron microscopy shows that the interface between these two phases is essentially commensurate, Figure 4c. This is important because it means that movement of this interface should be possible simply by the application of an electric field, as is indeed the case.[133] Second, and perhaps more importantly, the highly distorted R-phase in this ensemble, shows significantly enhanced ferromagnetism. This can be discerned from the x-ray magnetic circular dichroism-photoemission electron microscopy (XMCD-PEEM) image in Figure 4d. The R-phase appears in either bright or dark stripe-like contrast in such PEEM images, corresponding to the thin slivers being magnetized either along the x-ray polarization direction or anti-parallel to it.

A rough estimate of the magnetic moment of this highly strained R-phase (from the PEEM images as well as from superconducting quantum interference device magnetometry measurements) gives a local moment of the order of 25–35 emu/cc.[134] It is noteworthy that the canted moment of the R-phase (~6–8 emu/cc) is not observable by the XMCD technique due to the small magnitude of the moment. This enhanced magnetic moment in the highly strained R-phase disappears around 150°C.[134] Application of an electric field converts this mixed (R+T) phase into the T-phase, and the enhanced magnetic moment disappears; reversal of the electric field brings the mixed phase back accompanied by the magnetic moment in the distorted R-phase.[134]

There has been limited work on the tensile side of the $BiFeO_3$ strain phase diagram. It was, however, predicted, using phase-field calculations, that an orthorhombic (O) phase of $BiFeO_3$ should exist under sufficient tensile strain,[21] and recent work has shown that an O-phase can indeed be stabilized.[135] These observations on biaxially strained $BiFeO_3$ films raise several questions. First, what is the magnetic ground state of the various strained $BiFeO_3$ phases (e.g., do they have enhanced canting or exhibit spin glass behavior?). Second, given that spin-orbit coupling is the source of the canted moment in the bulk of $BiFeO_3$, can this enhanced moment be explained based on the strain and confinement imposed on the R-phase? Finally, what is the state of the Dzyaloshinskii–Moriya vector, the antisymmetric microscopic coupling between two localized magnetic moments, in such a strained system?

Strained $EuTiO_3$—Transforming a boring dielectric into the world's strongest ferroelectric ferromagnet

The strain game involving $EuTiO_3$ is another tale in which theory led the way to a remarkable strain-enabled discovery. The idea behind this new route to ferroelectric ferromagnets is that appropriate magnetically ordered insulators that are neither ferroelectric nor ferromagnetic, of which there are many, can be transmuted into ferroelectric ferromagnets. Fennie and Rabe predicted[136] that $EuTiO_3$, a normally boring paraelectric and antiferromagnetic insulator (in its unstrained bulk state), could be transformed using strain into the strongest known multiferroic with a spontaneous polarization and spontaneous magnetization each 100× superior to the reigning multiferroic it displaced, $Ni_3B_7O_{13}I$.[137,138]

The physics behind this discovery makes use of spin-lattice coupling as an additional parameter to influence the soft mode of an insulator on the verge of a ferroelectric transition.[139] The soft mode is the lowest frequency transverse optical phonon, which as it goes to zero results in the phase transition from a paraelectric to a ferroelectric. Appropriate materials for this (1) have a ground state that in the absence of strain is antiferromagnetic and paraelectric, (2) are on the brink of a ferroelectric transition, and (3) exhibit large spin-lattice coupling manifested by a significant decrease in permittivity as the material is cooled through its Néel temperature.[136] $EuTiO_3$ meets these criteria and has much in common with $SrTiO_3$ except that $EuTiO_3$ magnetically orders at 5 K due to the existence of localized 4*f* moments on the Eu^{2+} site.[140,141] Similar to $SrTiO_3$, strain can be used to soften the soft mode and drive it to a ferroelectric instability. In contrast to $SrTiO_3$, which is diamagnetic, the permittivity of bulk $EuTiO_3$ is strongly coupled with its magnetism, showing an abrupt decrease in permittivity at the onset of the antiferromagnetic Eu^{2+} ordering.[142] This indicates that the

https://doi.org/10.1557/mrs.2014.1 Published online by Cambridge University Press

soft mode frequency hardens when the spins order antiferromagnetically; conversely, it will soften if the spins order ferromagnetically. This extra interaction provides the coupling favoring a simultaneously ferroelectric and ferromagnetic ground state under sufficient strain in $EuTiO_3$.

Although testing this prediction seems straightforward, the groups who first tested it ran into an unforeseen complication: no matter what substrate they deposited $EuTiO_3$ on, it was ferromagnetic. With its identical lattice constant (both are 3.905 Å at room temperature), $SrTiO_3$ is an obvious substrate for the growth of unstrained epitaxial $EuTiO_3$ films. Surprisingly, as-grown $EuTiO_{3-\delta}$ thin films synthesized by pulsed-laser deposition (PLD) on (001) $SrTiO_3$ substrates exhibit expanded out-of-plane spacings (0.4% to 2% longer than bulk $EuTiO_3$)[143–146] and are ferromagnetic with a Curie temperature of about 5 K.[144,145]

Could the observed expanded lattice spacings in $EuTiO_{3-\delta}$ thin films be due to oxygen vacancies? The effect of oxygen deficiency on lattice constant has been studied in $EuTiO_{3-\delta}$ bulk samples down to the $EuTiO_{2.5}$ limit of the perovskite $EuTiO_{3-\delta}$ structure, and negligible (<0.5%) variation in the cubic lattice constant was found.[147,148] Oxygen vacancies alone are thus insufficient to explain the 2% variation in out-of-plane lattice spacings observed in epitaxial $EuTiO_{3-\delta}$ films grown on (001) $SrTiO_3$ by PLD.[144–146]

One possible explanation is that the ferromagnetism observed in epitaxial $EuTiO_3$ films prepared by PLD on $SrTiO_3$ arises from extrinsic effects, masking the intrinsic properties of $EuTiO_3$ thin films. Extrinsic effects are known to occur in thin films, particularly for deposition methods involving energetic species, which can induce defects. Another factor favoring defect introduction is the relatively low growth temperatures common for oxide thin-film growth, enabling defects to be frozen in. For example, some epitaxial $SrTiO_3$ films grown on $SrTiO_3$ substrates by PLD have been reported to be ferroelectric,[149] in striking contrast to the intrinsic nature of unstrained $SrTiO_3$, which is not ferroelectric at any temperature.[150] Homoepitaxial $SrTiO_3$ films grown by PLD are also known to exhibit lattice spacings that deviate significantly from the $SrTiO_3$ substrates they are grown on,[151–153] although bulk $SrTiO_{3-\delta}$ (in either single crystal or polycrystalline form) exhibits negligible variation in its cubic lattice constant up to the $SrTiO_{2.5}$ limit[154,155] of the perovskite $SrTiO_{3-\delta}$ structure. The sensitivity of $EuTiO_3$ that made it an appropriate material to transmute via strain into a multiferroic also makes it quite sensitive to defects. To overcome this issue and examine the intrinsic effect of strain on $EuTiO_3$, a more delicate deposition technique was needed.

In contrast to PLD, homoepitaxial $SrTiO_3$ films grown by MBE[156] show bulk behavior and none of the unusual effects reported in homoepitaxial $SrTiO_3$ films grown by PLD.[149,151–153] Indeed unstrained, stoichiometric $EuTiO_3$ thin films grown by MBE on (001) $SrTiO_3$ have the same lattice constant as bulk $EuTiO_3$ and are antiferromagnetic.[157] Seeing that MBE can produce $EuTiO_3$ films with intrinsic properties in their unstrained state, MBE was used to test Fennie and Rabe's strained $EuTiO_3$ predictions.[136] Commensurate $EuTiO_3$ films were grown on three substrates: (001) LSAT, (001) $SrTiO_3$, and (110) $DyScO_3$ to impart –0.9%, 0%, and +1.1% biaxial

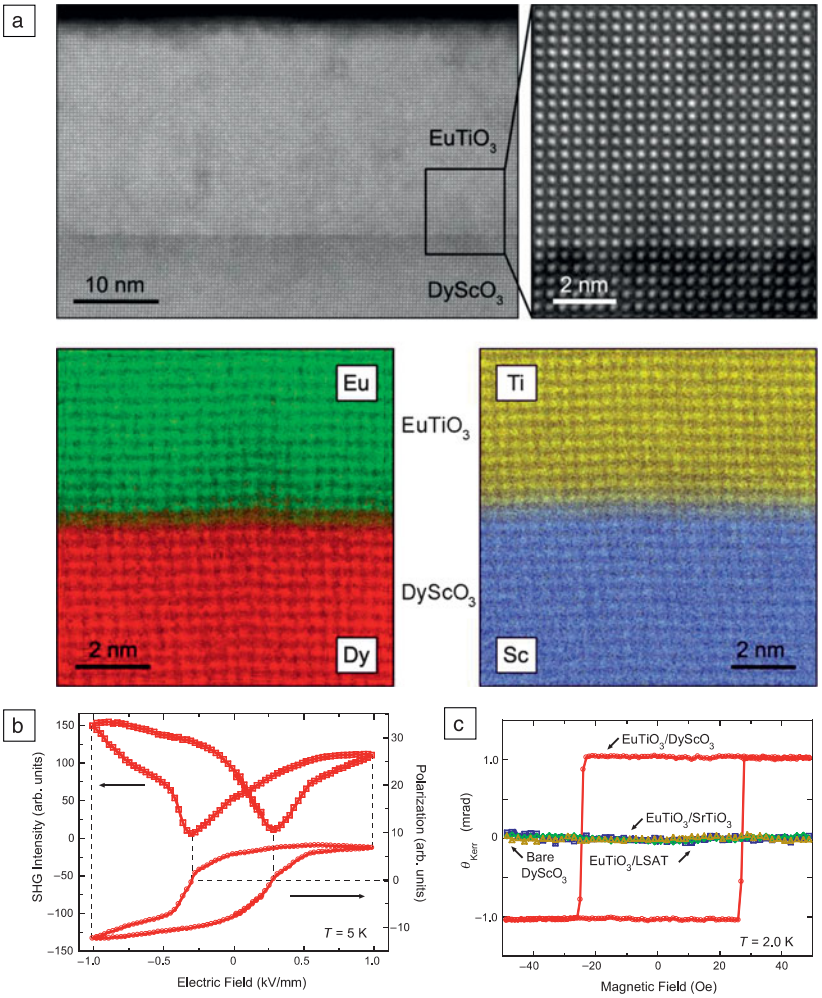


Figure 5. (a) Elemental maps of europium and dysprosium observed by scanning transmission electron microscopy-electron energy loss spectroscopy on a 22-nm-thick commensurate $EuTiO_3/DyScO_3$ film, confirming an abrupt $EuTiO_3/DyScO_3$ interface with the correct oxidation states. Observation of (b) ferroelectricity by second harmonic generation and (c) ferromagnetism by magneto-optical Kerr effect in this same strained $EuTiO_3$ grown on (110) $DyScO_3$, confirming predictions that under sufficient biaxial strain, $EuTiO_3$ becomes multiferroic. Control samples with zero ($EuTiO_3/SrTiO_3$) or opposite ($EuTiO_3/LSAT$)) strain are consistent with the theoretically predicted strain phase diagram for $EuTiO_3$. LSAT, $(LaAlO_3)_{0.29}-(SrAl_{1/2}Ta_{1/2}O_3)_{0.71}$. Reprinted with permission from Reference 16. © 2010 Nature Publishing Group.

https://doi.org/10.1557/mrs.2014.1 Published online by Cambridge University Press

strain, respectively. Using scanning transmission electron microscopy with electron energy loss spectroscopy (STEM-EELS), the oxidation state of the film constituents and the abruptness of the interface between the film and substrate was checked with atomic resolution and chemical specificity (**Figure 5**a). Experimental measurements utilizing second harmonic generation (SHG) and magneto-optic Kerr effect (MOKE) confirmed that the $EuTiO_3$ grown on (110) $DyScO_3$ was simultaneously ferroelectric (Figure 5b) and ferromagnetic (Figure 5c), while on the other substrates it was not, in agreement with theory[136] and resulting in the strongest multiferroic material known today.[16]

There are many other exciting predictions that remain to be verified of even stronger and higher temperature ferroelectric ferromagnets in strained $SrMnO_3$,[158] and EuO,[159] as well as the prediction that an electric field on the order of 10^5 V cm^{-1} can be used to turn on ferromagnetism in $EuTiO_3$ when it is poised on the verge of such a phase transition via strain.[136] It was recently shown that through the application of an electric field, the antiferromagnetic ground state of $EuTiO_3$, strained to be close to where it would have a ferromagnetic ground state (but still on the antiferromagnetic side), can be electrically tuned to the verge of the ferromagnetic state.[160] Turning on magnetism in a material by applying an electric field to it remains an open challenge. Such an important milestone would be a key advance to the field of ferroics, both scientifically and technologically.

Electronics has flourished because of the ability to route voltages with ease and on extremely small scales. If magnetism could be similarly controlled and routed, it would impact memory devices, spin valves, and many other spintronics devices and make numerous hybrid devices possible.

Strained $Sr_{n+1}Ti_nO_{3n+1}$—Creating a tunable dielectric with record performance

Strain has also been used to create a new family of tunable microwave dielectrics, which due to their low dielectric loss have a figure of merit at room temperature that rivals those of all such known materials.[161] In contrast to standard (textbook) dielectrics, whose dielectric displacement (**D**) as a function of applied electric field (**E**) can be described by the linear equation

$$\mathbf{D} = \varepsilon_0 \boldsymbol{K} \mathbf{E}, \qquad (1)$$

where ε_0 is the permittivity of free space and $\boldsymbol{K}$ is the dielectric constant of the material, a tunable dielectric has a highly nonlinear relationship between **D** and **E**. The nonlinearity results in the effective dielectric constant of the material ($\mathbf{D}/\varepsilon_0\mathbf{E}$) behaving not as a constant, but changing greatly with **E**; changes of tens of percent in the dielectric "constant" are common in tunable dielectrics at high **E**. This nonlinearity can be described by adding higher order terms to Equation 1. In tensor form, this more general relationship is

$$D_i = \varepsilon_0 K_{ij} E_j + \varepsilon_{ijk} E_j E_k + \varepsilon_{ijk\ell} E_j E_k E_\ell + \ldots, \qquad (2)$$

where ε_{ijk} and $\varepsilon_{ijk\ell}$ are higher order permittivity coefficients.

Highly nonlinear dielectrics, including the most extensively studied material with such properties, $Ba_xSr_{1-x}TiO_3$,[162–165] are found in displacive ferroelectric systems at temperatures just above the paraelectric-to-ferroelectric transition temperature.[162,165] These tunable dielectrics are normally used in their paraelectric state to avoid the dielectric losses that would occur in the ferroelectric state due to the motion of domain walls. Although thin films provide an excellent geometry for the application of high **E** at low applied voltages, $Ba_xSr_{1-x}TiO_3$ films unfortunately suffer significant dielectric losses arising from defects; the dielectric loss in today's best $Ba_xSr_{1-x}TiO_3$ tunable dielectrics films at GHz frequencies is about an order of magnitude worse than the best $Ba_xSr_{1-x}TiO_3$ in bulk form.[165]

A new approach to tunable microwave dielectrics is to take a system with exceptionally low loss and introduce a ferroelectric instability into it using strain. The appeal of this approach is that it can be applied to systems that are known to have exceptionally low dielectric loss, particularly in thin-film form. Such systems do not need to have a ferroelectric instability in their unstrained form; strain can be used to help impart the ferroelectric instability. This relaxed design constraint greatly increases the number of eligible systems that could yield improved performance over the best of today's known tunable dielectrics.

This approach has been applied to $Sr_{n+1}Ti_nO_{3n+1}$ phases—where $(SrO)_2$ crystallographic shear[166,167] planes provide an alternative to point-defect formation for accommodating nonstoichiometry.[168,169] These phases are known to have low dielectric loss,[170,171] even in thin-film form.[172] In their unstrained state, these phases are centrosymmetric, and thus lack a ferroelectric instability.

The strain game in combination with control of the distance between the $(SrO)_2$ planes in $Sr_{n+1}Ti_nO_{3n+1}$ phases can, however, induce a ferroelectric instability.[161,173] The emergence of this ferroelectric instability in $Sr_{n+1}Ti_nO_{3n+1}$ phases commensurately strained in biaxial tension to (110) $DyScO_3$ substrates (about 1% biaxial tension) can be seen in **Figure 6**a. For $n \geq 3$, a ferroelectric instability is evident from the double-well energy potential of the ion displacements, and this double-well becomes deeper with increasing n. A deeper well corresponds to the ferroelectric instability occurring at higher temperature until, by $n = 6$, it is just below room temperature.[161]

The low loss of this tunable dielectric at high frequencies is evident from Figure 6b, where both the real and imaginary parts of the in-plane dielectric constant K_{11} are shown over a frequency range spanning more than eight orders of magnitude and up to 125 GHz.[161] Only at these highest frequencies can the dielectric loss be seen. This low loss yields unparalleled performance at room temperature for these new tunable dielectrics.[164] The reason for the low dielectric loss, far lower than today's best $Ba_xSr_{1-x}TiO_3$ tunable dielectrics at GHz frequencies, is believed to be related to the propensity of $Sr_{n+1}Ti_nO_{3n+1}$ phases to form $(SrO)_2$ planar defects in response to

https://doi.org/10.1557/mrs.2014.1 Published online by Cambridge University Press

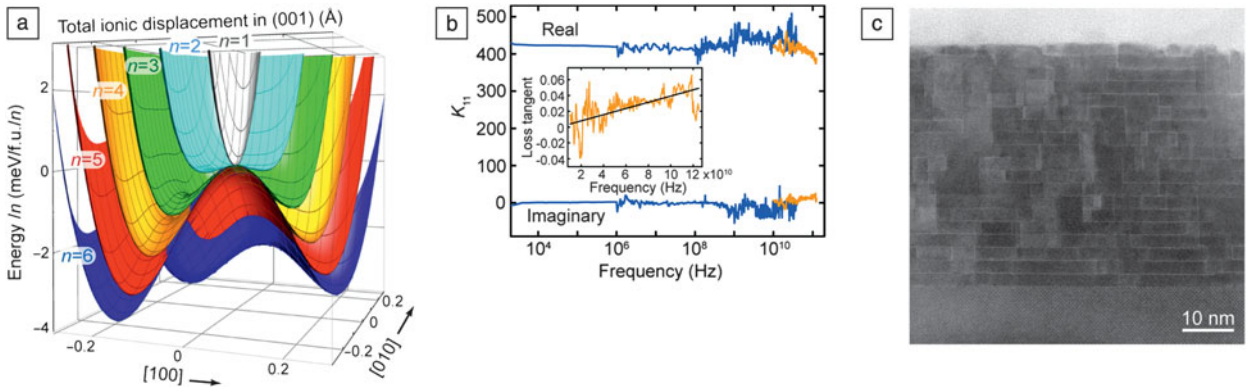


Figure 6. (a) First-principles calculations showing how the index n of $Sr_{n+1}Ti_nO_{3n+1}$ phases strained commensurately to (110) $DyScO_3$ substrates can be used to control the local ferroelectric instability. Plotted is the energy (per n) with respect to the nonpolar state of $Sr_{n+1}Ti_nO_{3n+1}$ phases for polar distortions in the (001) plane. (b) The real and imaginary parts of the in-plane dielectric constant (K_{11}) of an n = 6 $Sr_{n+1}Ti_nO_{3n+1}$ film grown on (110) $DyScO_3$ as a function of frequency. The inset shows the film loss tangent on a linear frequency scale in the gigahertz frequency regime along with a linear fit. (c) Bright-field scanning transmission electron microscopy image of an n = 6 $Sr_{n+1}Ti_nO_{3n+1}$ film grown on (110) $DyScO_3$. $Sr_{n+1}Ti_nO_{3n+1}$ phases can readily accommodate nonstoichiometry by the formation of $(SrO)_2$ double layers, the bright horizontal and vertical running layers in this image. Reprinted with permission from Reference 161. © 2013 Nature Publishing Group.

local stoichiometry deviations rather than point defects.[168,169] These $(SrO)_2$ double layers show up as bright layers in the STEM image of an n = 6 $Sr_{n+1}Ti_nO_{3n+1}$ film in Figure 6c. This is in contrast to the high point-defect concentrations that perovskite films like $SrTiO_3$ can incorporate in thin-film form;[75,156] such point defects could be the reason that $Ba_xSr_{1-x}TiO_3$ tunable dielectric films have significantly higher dielectric losses than bulk $Ba_xSr_{1-x}TiO_3$.[165]

Other ways oxides can react to strain

As the examples described in this article show, the strain game can be a powerful control parameter for enhancing the properties of ferroic oxides. It is important to consider, however, other ways in which a complex oxide might react to strain. Should there be an energetically more favorable route to accommodate the imposed strain, the system might take it. Examples include the possibility that the imposed strain will lead to changes in film composition, microstructure, or crystal structure (e.g., ordering [or disordering] of cations, anions, or their vacancies,[174,175] atom clustering, the stabilization of other polymorphs, or rotations of the oxygen coordination polyhedra[176–178]) rather than simply dilating or compressing the spacings between the atoms in the unstrained structure equally. Octahedral rotation patterns from underlying layers and substrates can be imparted into films over distances of several nanometers and can thus complicate a simple biaxial strain picture. An example is the creation of T-phase $BiFeO_3$ at relatively low biaxial strain (–1.4%, where the $BiFeO_3$ should be monoclinic), due to the competition between different octahedral rotation patterns in the film and in the substrate.[179] Such chemical and structural changes may also cause dramatic changes in properties, for better or worse, but it is important to distinguish the underlying causes of the changes in properties.

Advances in electron microscopy have been particularly beneficial in identifying these underlying causes (see the Hÿtch and Minor article in this issue). With respect to ferroics, recent advances enabling polarization mapping on the atomic scale,[180–183] octahedral rotation imaging,[184] and improved STEM-EELS analysis[185] are invaluable in separating true strain effects from changes in composition, structure, and microstructure that can occur to mitigate against a strain effect. These techniques have the potential to visualize closure domains in ferroelectrics,[182,183] usual domain walls with mixed Bloch–Néel–Ising character in strained ferroelectric superlattices,[186] and the exciting possibility of a dipole-dipole coupling analog of exchange-spring magnets[187,188] recently predicted to occur in strained ferroelectric systems.[189]

Other intriguing predictions, including using strain to poise a material (e.g., $SrCoO_3$[190]) on the brink of a metal-insulator transition, which could then be turned on or off through the application of an electric or magnetic field or even a small additional strain, are relevant to emerging piezotronic devices.[191,192]

Outlook

Elastic strain engineering of ferroics with the perovskite structure has been the most pursued to date. Yet there are many other fascinating oxides that either have a ferroic ground state or are borderline ferroic materials that might be enticed into a ferroic ground state with strain. Such non-perovskite structural families that are relevant include chrysoberyl Cr_2BeO_4,[193] pyrochlore $Ho_2Ti_2O_7$,[194] $YMnO_3$,[195,196] $MnWO_4$,[197] delafossite $CuFeO_2$,[198] CuO,[199] and hexaferrite $Sr_3Co_2Fe_{24}O_{41}$.[200] These systems are generally ignored by the thin-film community and have been the focus of the single crystal ferroic community. We believe the issue is the lack of suitable substrates for these latter structures; removing this roadblock would unleash a

https://doi.org/10.1557/mrs.2014.1 Published online by Cambridge University Press

huge opportunity in strain engineering for the future. Thin films also have the technological advantage of lower switching voltages and the ability to integrate them into more sophisticated heterostructures, as are relevant for devices.

Imagine the opportunities for strain engineering that substrates for the non-perovskite systems would bring. Substrates for $YMnO_3$ would enable more variants of hexagonal manganite ferroics to be constructed. These variants include not only known materials, but metastable polymorphs (e.g., $LuFeO_3$ that is isostructural to $YMnO_3$ rather than its stable centrosymmetric perovskite form)[124,201,202] by utilizing lattice misfit strain energies and interfacial energies to favor the desired metastable phase over the equilibrium phase (epitaxial stabilization),[203–206] or the prospect of interfacial multiferroicity that has been predicted to emerge in superlattices between centrosymmetric components.[207,208]

Similarly, substrates with the $LiNbO_3$ structure would enable the growth of the $LiNbO_3$-polymorph of $FeTiO_3$ and related multiferroics.[209,210] A range of appropriate substrates, like the range of substrates available for perovskites shown in Figure 1d, for each ferroic system of interest would allow the thin-film tricks of strain engineering,[12–16] epitaxial stabilization,[203–206] dimensional confinement,[161,173] polarization engineering,[112,211] and superlattice formation[60,103–114,117–119,207,208] to be freely applied to a much larger set of ferroic building blocks. Strain engineering of ferroic oxides is in its infancy and considering its brief, but vibrant past, a brilliant future awaits.

Acknowledgments

We gratefully acknowledge our colleagues and collaborators for sharing their insights and helping us to explore and better understand the exciting area of elastically strained ferroic oxide films. We especially thank the groups of E. Arenholz, M. Bedzyk, M.D. Biegalski, D.H.A. Blank, D.A. Bonnell, J.C. Booth, J.D. Brock, L.E. Cross, C.B. Eom, J.W. Freeland, P. Ghosez, P.C. Hammel, M.E. Hawley, E. Johnston-Halperin, S. Kamba, S.W. Kirchoefer, J. Levy, Yulan Li, T.E. Mallouk, J. Mannhart, L.W. Martin, K. Peters, K.M. Rabe, J.M. Rondinelli, P.J. Ryan, P. Schiffer, J. Schubert, N.A. Spaldin, S.K. Streiffer, A.K. Tagantsev, I. Takeuchi, D.A. Tenne, J.-M. Triscone, S. Trolier-McKinstry, D. Vanderbilt, J.C. Woicik, and X.X. Xi. L.Q.C., C.J.F., V.G., X.Q.P., D.G.S., and R.R. gratefully acknowledge financial support from the National Science Foundation (NSF) under Grant No. DMR-0820404. D.G.S. also acknowledges NSF Grant DMR-0948036. R.R. acknowledges sustained support from the US Department of Energy under Contract No. DE-AC0205CH11231.

References

1. A.E. Lindh, in *Nobel Lectures in Physics 1942–1962* (World Scientific, Singapore, 1998), pp. 49–52.
2. J.M. Lock, *Philos. Trans. R. Soc. London, Ser. A* **208**, 391 (1951).
3. P.W. Forsbergh Jr., *Phys. Rev.* **93**, 686 (1954).
4. L.D. Nguyen, A.S. Brown, M.A. Thompson, L.M. Jelloian, *IEEE Trans. Electron Devices* **39**, 2007 (1992).
5. J. Welser, J.L. Hoyt, J.F. Gibbons, *IEEE Electron Device Lett.* **15**, 100 (1994).
6. W. Shockley, J. Bardeen, *Phys. Rev.* **77**, 407 (1950).
7. H. Sato, M. Naito, *Physica C* **274**, 221 (1997).
8. I. Bozovic, G. Logvenov, I. Belca, B. Narimbetov, I. Sveklo, *Phys. Rev. Lett.* **89**, 107001 (2002).
9. R.S. Beach, J.A. Borchers, A. Matheny, R.W. Erwin, M.B. Salamon, B. Everitt, K. Pettit, J.J. Rhyne, C.P. Flynn, *Phys. Rev. Lett.* **70**, 3502 (1993).
10. Q. Gan, R.A. Rao, C.B. Eom, J.L. Garrett, M. Lee, *Appl. Phys. Lett.* **72**, 978 (1998).
11. D. Fuchs, E. Arac, C. Pinta, S. Schuppler, R. Schneider, H.v. Löhneysen, *Phys. Rev. B.* **77**, 014434 (2008).
12. J.H. Haeni, P. Irvin, W. Chang, R. Uecker, P. Reiche, Y.L. Li, S. Choudhury, W. Tian, M.E. Hawley, B. Craigo, A.K. Tagantsev, X.Q. Pan, S.K. Streiffer, L.Q. Chen, S.W. Kirchoefer, J. Levy, D.G. Schlom, *Nature* **430**, 758 (2004).
13. K.J. Choi, M.D. Biegalski, Y.L. Li, A. Sharan, J. Schubert, R. Uecker, P. Reiche, Y.B. Chen, X.Q. Pan, V. Gopalan, L.-Q. Chen, D.G. Schlom, C.B. Eom, *Science* **306**, 1005 (2004).
14. D.G. Schlom, L.Q. Chen, C.B. Eom, K.M. Rabe, S.K. Streiffer, J.-M. Triscone, *Annu. Rev. Mater. Res.* **37**, 589 (2007).
15. M.P. Warusawithana, C. Cen, C.R. Sleasman, J.C. Woicik, Y.L. Li, L.F. Kourkoutis, J.A. Klug, H. Li, P. Ryan, L.-P. Wang, M. Bedzyk, D.A. Muller, L.Q. Chen, J. Levy, D.G. Schlom, *Science* **324**, 367 (2009).
16. J.H. Lee, L. Fang, E. Vlahos, X. Ke, Y.W. Jung, L.F. Kourkoutis, J.-W. Kim, P.J. Ryan, T. Heeg, M. Roeckerath, V. Goian, M. Bernhagen, R. Uecker, P.C. Hammel, K.M. Rabe, S. Kamba, J. Schubert, J.W. Freeland, D.A. Muller, C.J. Fennie, P. Schiffer, V. Gopalan, E. Johnston-Halperin, D.G. Schlom, *Nature* **466**, 954 (2010).
17. C. Adamo, X. Ke, H.Q. Wang, H.L. Xin, T. Heeg, M.E. Hawley, W. Zander, J. Schubert, P. Schiffer, D.A. Muller, L. Maritato, D.G. Schlom, *Appl. Phys. Lett.* **95**, 112504 (2009).
18. H. Béa, B. Dupé, S. Fusil, R. Mattana, E. Jacquet, B. Warot-Fonrose, F. Wilhelm, A. Rogalev, S. Petit, V. Cros, A. Anane, F. Petroff, K. Bouzehouane, G. Geneste, B. Dkhil, S. Lisenkov, I. Ponomareva, L. Bellaiche, M. Bibes, A. Barthélémy, *Phys. Rev. Lett.* **102**, 217603 (2009).
19. I.C. Infante, S. Lisenkov, B. Dupé, M. Bibes, S. Fusil, E. Jacquet, G. Geneste, S. Petit, A. Courtial, J. Juraszek, L. Bellaiche, A. Barthélémy, B. Dkhil, *Phys. Rev. Lett.* **105**, 057601 (2010).
20. Z. Chen, Z. Luo, C. Huang, Y. Qi, P. Yang, L. You, C. Hu, T. Wu, J. Wang, C. Gao, T. Sritharan, L. Chen, *Adv. Funct. Mater.* **21**, 133 (2011).
21. R.J. Zeches, M.D. Rossell, J.X. Zhang, A.J. Hatt, Q. He, C.-H. Yang, A. Kumar, C.H. Wang, A. Melville, C. Adamo, G. Sheng, Y.-H. Chu, J.F. Ihlefeld, R. Erni, C. Ederer, V. Gopalan, L.Q. Chen, D.G. Schlom, N.A. Spaldin, L.W. Martin, R. Ramesh, *Science* **326**, 977 (2009).
22. P. Chen, N.J. Podraza, X.S. Xu, A. Melville, E. Vlahos, V. Gopalan, R. Ramesh, D.G. Schlom, J.L. Musfeldt, *Appl. Phys. Lett.* **96**, 131907 (2010).
23. H.M. Christen, J.H. Nam, H.S. Kim, A.J. Hatt, N.A. Spaldin, *Phys. Rev. B* **83**, 144107 (2011).
24. L.W. Martin, D.G. Schlom, *Curr. Opin. Solid State Mater. Sci.* **16**, 199 (2012).
25. A.A. Griffith, *Philos. Trans. R. Soc. London, Ser. A* **221**, 163 (1920).
26. E. Klokholm, J.W. Matthews, A.F. Mayadas, J. Angilello, in *Magnetism and Magnetic Materials*, C.D. Graham Jr., J.J. Rhyne, Eds. (American Institute of Physics, New York, 1972), pp. 105–109.
27. L.B. Freund, S. Suresh, *Thin Film Materials: Stress, Defect Formation and Surface Evolution* (Cambridge University Press, Cambridge, 2003), pp. 60–83, 283–290, 396–416.
28. N.A. Pertsev, A.K. Tagantsev, N. Setter, *Phys. Rev. B* **61**, R825 (2000).
29. N.A. Pertsev, A.K. Tagantsev, N. Setter, *Phys. Rev. B* **65**, 219901 (2002).
30. A.F. Devonshire, *Philos. Mag.* **3** (Suppl.), 85 (1954).
31. A. Antons, J.B. Neaton, K.M. Rabe, D. Vanderbilt, *Phys. Rev. B* **71**, 024102 (2005).
32. Y.L. Li, S. Choudhury, J.H. Haeni, M.D. Biegalski, A. Vasudevarao, A. Sharan, H.Z. Ma, J. Levy, V. Gopalan, S. Trolier-McKinstry, D.G. Schlom, Q.X. Jia, L.Q. Chen, *Phys. Rev. B* **73**, 184112 (2006).
33. C.L. Canedy, H. Li, S.P. Alpay, L. Salamanca-Riba, A.L. Roytburd, R. Ramesh, *Appl. Phys. Lett.* **77**, 1695 (2000).
34. I.B. Misirlioglu, A.L. Vasiliev, M. Aindow, S.P. Alpay, R. Ramesh, *Appl. Phys. Lett.* **84**, 1742 (2004).
35. M.-W. Chu, I. Szafraniak, R. Scholz, C. Harnagea, D. Hesse, M. Alexe, U. Gösele, *Nature Mater.* **3**, 87 (2004).
36. S.P. Alpay, I.B. Misirlioglu, V. Nagarajan, R. Ramesh, *Appl. Phys. Lett.* **85**, 2044 (2004).
37. V. Nagarajan, C.L. Jia, H. Kohlstedt, R. Waser, I.B. Misirlioglu, S.P. Alpay, R. Ramesh, *Appl. Phys. Lett.* **86**, 192910 (2005).
38. M.D. Biegalski, D.D. Fong, J.A. Eastman, P.H. Fuoss, S.K. Streiffer, T. Heeg, J. Schubert, W. Tian, C.T. Nelson, X.Q. Pan, M.E. Hawley, M. Bernhagen, P. Reiche, R. Uecker, S. Trolier-McKinstry, D.G. Schlom, *J. Appl. Phys.* **104**, 114109 (2008).
39. R. Uecker, H. Wilke, D.G. Schlom, B. Velickov, P. Reiche, A. Polity, M. Bernhagen, M. Rossberg, *J. Cryst. Growth* **295**, 84 (2006).

https://doi.org/10.1557/mrs.2014.1 Published online by Cambridge University Press

40. R. Uecker, B. Velickov, D. Klimm, R. Bertram, M. Bernhagen, M. Rabe, M. Albrecht, R. Fornari, D.G. Schlom, *J. Cryst. Growth* **310**, 2649 (2008).
41. R. Uecker, D. Klimm, R. Bertram, M. Bernhagen, I. Schulze-Jonack, M. Brützam, A. Kwasniewski, T.M. Gesing, D.G. Schlom, *Acta Phys. Pol. A* **124**, 295 (2013).
42. A. Lempicki, M.H. Randles, D. Wisniewski, M. Balcerzyk, C. Brecher, A.J. Wojtowicz, *IEEE Trans. Nucl. Sci.* **42**, 280 (1995).
43. A.G. Petrosyan, G.O. Shirinyan, C. Pedrini, C. Durjardin, K.L. Ovanesyan, R.G. Manucharyan, T.I. Butaeva, M.V. Derzyan, *Cryst. Res. Technol.* **33**, 241 (1998).
44. H. Asano, S. Kubo, O. Michikami, M. Satoh, T. Konaka, *Jpn. J. Appl. Phys., Part 2* **29**, L1452 (1990).
45. R. Brown, V. Pendrick, D. Kalokitis, B.H.T. Chai, *Appl. Phys. Lett.* **57**, 1351 (1990).
46. Y. Miyazawa, H. Toshima, S. Morita, *J. Cryst. Growth* **128**, 668 (1993).
47. G.W. Berkstresser, A.J. Valentino, C.D. Brandle, *J. Cryst. Growth* **109**, 467 (1991).
48. G.W. Berkstresser, A.J. Valentino, C.D. Brandle, *J. Cryst. Growth* **128**, 684 (1993).
49. S. Hontsu, J. Ishii, T. Kawai, S. Kawai, *Appl. Phys. Lett.* **59**, 2886 (1991).
50. D. Mateika, H. Kohler, H. Laudan, E. Volkel, *J. Cryst. Growth* **109**, 447 (1991).
51. R.W. Simon, C.E. Platt, A.E. Lee, G.S. Lee, K.P. Daly, M.S. Wire, J.A. Luine, M. Urbanik, *Appl. Phys. Lett.* **53**, 2677 (1988).
52. G.W. Berkstresser, A.J. Valentino, C.D. Brandle, *J. Cryst. Growth* **109**, 457 (1991).
53. B.C. Chakoumakos, D.G. Schlom, M. Urbanik, J. Luine, *J. Appl. Phys.* **83**, 1979 (1998).
54. R.L. Sandstrom, E.A. Giess, W.J. Gallagher, A. Segmüller, E.I. Cooper, M.F. Chisholm, A. Gupta, S. Shinde, R.B. Laibowitz, *Appl. Phys. Lett.* **53**, 1874 (1988).
55. L. Merker, US Patent No. 2,684,910 (27 July 1954).
56. J.G. Bednorz, H.J. Scheel, *J. Cryst. Growth* **41**, 5 (1977).
57. P.I. Nabokin, D. Souptel, A.M. Balbashov, *J. Cryst. Growth* **250**, 397 (2003).
58. H.J. Scheel, J.G. Bednorz, P. Dill, *Ferroelectrics* **13**, 507 (1976).
59. S.-G. Lim, S. Kriventsov, T.N. Jackson, J.H. Haeni, D.G. Schlom, A.M. Balbashov, R. Uecker, P. Reiche, J.L. Freeouf, G. Lucovsky, *J. Appl. Phys.* **91**, 4500 (2002).
60. A. Soukiassian, W. Tian, V. Vaithyanathan, J.H. Haeni, L.Q. Chen, X.X. Xi, D.G. Schlom, D.A. Tenne, H.P. Sun, X.Q. Pan, K.J. Choi, C.B. Eom, Y.L. Li, Q.X. Jia, C. Constantin, R.M. Feenstra, M. Bernhagen, P. Reiche, R. Uecker, *J. Mater. Res.* **23**, 1417 (2008).
61. R. Feenstra, L.A. Boatner, J.D. Budai, D.K. Christen, M.D. Galloway, D.B. Poker, *Appl. Phys. Lett.* **54**, 1063 (1989).
62. J.C. Yang, Q. He, S.J. Suresha, C.Y. Kuo, C.Y. Peng, R.C. Haislmaier, M.A. Motyka, G. Sheng, C. Adamo, H.J. Lin, Z. Hu, L. Chang, L.H. Tjeng, E. Arenholz, N.J. Podraza, M. Bernhagen, R. Uecker, D.G. Schlom, V. Gopalan, L.Q. Chen, C.T. Chen, R. Ramesh, Y.H. Chu, *Phys. Rev. Lett.* **109**, 247606 (2012).
63. S. Coh, T. Heeg, J.H. Haeni, M.D. Biegalski, J. Lettieri, L.F. Edge, K.E. O'Brien, M. Bernhagen, P. Reiche, R. Uecker, S. Trolier-McKinstry, D.G. Schlom, D. Vanderbilt, *Phys. Rev. B* **82**, 064101 (2010).
64. K.L. Ovanesyan, A.G. Petrosyan, G.O. Shirinyan, C. Pedrini, L. Zhang, *J. Cryst. Growth* **198**, 497 (1999).
65. M.D. Biegalski, Y. Jia, D.G. Schlom, S. Trolier-McKinstry, S.K. Streiffer, V. Sherman, R. Uecker, P. Reiche, *Appl. Phys. Lett.* **88**, 192907 (2006).
66. J.F. Ihlefeld, W. Tian, Z.-K. Liu, W.A. Doolittle, M. Bernhagen, P. Reiche, R. Uecker, R. Ramesh, D.G. Schlom, *IEEE Trans. Ultrason. Ferroelectr. Freq. Control* **56**, 1528 (2009).
67. J.H. Lee, X. Ke, R. Misra, J.F. Ihlefeld, X.S. Xu, Z.G. Mei, T. Heeg, M. Roeckerath, J. Schubert, Z.K. Liu, J.L. Musfeldt, P. Schiffer, D.G. Schlom, *Appl. Phys. Lett.* **96**, 262905 (2010).
68. P. Irvin, J. Levy, J.H. Haeni, D.G. Schlom, *Appl. Phys. Lett.* **88**, 042902 (2006).
69. H.Z. Ma, J. Levy, M.D. Biegalski, S. Trolier-McKinstry, D.G. Schlom, *J. Appl. Phys.* **105**, 014102 (2009).
70. A. Vasudevarao, A. Kumar, L. Tian, J.H. Haeni, Y.L. Li, C.-J. Eklund, Q.X. Jia, R. Uecker, P. Reiche, K.M. Rabe, L.Q. Chen, D.G. Schlom, V. Gopalan, *Phys. Rev. Lett.* **97**, 257602 (2006).
71. A. Vasudevarao, S. Denev, M.D. Biegalski, Y.L. Li, L.Q. Chen, S. Trolier-McKinstry, D.G. Schlom, V. Gopalan, *Appl. Phys. Lett.* **92**, 192902 (2008).
72. S. Denev, A. Kumar, M.D. Biegalski, H.W. Jang, C.M. Folkman, A. Vasudevarao, Y. Han, I.M. Reaney, S. Trolier-McKinstry, C.B. Eom, D.G. Schlom, V. Gopalan, *Phys. Rev. Lett.* **100**, 257601 (2008).
73. M.D. Biegalski, E. Vlahos, G. Sheng, Y.L. Li, M. Bernhagen, P. Reiche, R. Uecker, S.K. Streiffer, L.Q. Chen, V. Gopalan, D.G. Schlom, S. Trolier-McKinstry, *Phys. Rev. B* **79**, 224117 (2009).
74. D. Nuzhnyy, J. Petzelt, S. Kamba, P. Kužel, C. Kadlec, V. Bovtun, M. Kempa, J. Schubert, C.M. Brooks, D.G. Schlom, *Appl. Phys. Lett.* **95**, 232902 (2009).
75. C.H. Lee, V. Skoromets, M.D. Biegalski, S. Lei, R. Haislmaier, M. Bernhagen, R. Uecker, X.X. Xi, V. Gopalan, X. Martí, S. Kamba, P. Kužel, D.G. Schlom, *Appl. Phys. Lett.* **102**, 082905 (2013).
76. K.J. Hubbard, D.G. Schlom, *J. Mater. Res.* **11**, 2757 (1996).
77. D.G. Schlom, S. Guha, S. Datta, *MRS Bull.* **33**, 1017 (2008).
78. L.F. Kourkoutis, C.S. Hellberg, V. Vaithyanathan, H. Li, M.K. Parker, K.E. Andersen, D.G. Schlom, D.A. Muller, *Phys. Rev. Lett.* **100**, 036101 (2008).
79. H. Li, X. Hu, Y. Wei, Z. Yu, X. Zhang, R. Droopad, A.A. Demkov, J. Edwards, K. Moore, W. Ooms, J. Kulik, P. Fejes, *J. Appl. Phys.* **93**, 4521 (2003).
80. M. Kawasaki, K. Takahashi, T. Maeda, R. Tsuchiya, M. Shinohara, O. Ishiyama, T. Yonezawa, M. Yoshimoto, H. Koinuma, *Science* **266**, 1540 (1994).
81. G. Koster, B.L. Kropman, G.J.H.M. Rijnders, D.H.A. Blank, H. Rogalla, *Appl. Phys. Lett.* **73**, 2920 (1998).
82. A.G. Schrott, J.A. Misewich, M. Copel, D.W. Abraham, Y. Zhang, *Appl. Phys. Lett.* **79**, 1786 (2001).
83. A. Biswas, P.B. Rossen, C.H. Yang, W. Siemons, M.H. Jung, I.K. Yang, R. Ramesh, Y.H. Jeong, *Appl. Phys. Lett.* **98**, 051904 (2011).
84. J. Chang, Y.-S. Park, S.-K. Kim, *Appl. Phys. Lett.* **92**, 152910 (2008).
85. J.L. Blok, X. Wan, G. Koster, D.H.A. Blank, G. Rijnders, *Appl. Phys. Lett.* **99**, 151917 (2011).
86. T. Ohnishi, K. Takahashi, M. Nakamura, M. Kawasaki, M. Yoshimoto, H. Koinuma, *Appl. Phys. Lett.* **74**, 2531 (1999).
87. J.H. Ngai, T.C. Schwendemann, A.E. Walker, Y. Segal, F.J. Walker, E.I. Altman, C.H. Ahn, *Adv. Mater.* **22**, 2945 (2010).
88. J.E. Kleibeuker, G. Koster, W. Siemons, D. Dubbink, B. Kuiper, J.L. Blok, C.-H. Yang, J. Ravichandran, R. Ramesh, J.E. ten Elshof, D.H.A. Blank, G. Rijnders, *Adv. Funct. Mater.* **20**, 3490 (2010).
89. J.E. Kleibeuker, B. Kuiper, S. Harkema, D.H.A. Blank, G. Koster, G. Rijnders, P. Tinnemans, E. Vlieg, P.B. Rossen, W. Siemons, G. Portale, J. Ravichandran, J.M. Szepieniec, R. Ramesh, *Phys. Rev. B* **85**, 165413 (2012).
90. H.-J. Bae, J. Sigman, D.P. Norton, L.A. Boatner, *Appl. Surf. Sci.* **241**, 271 (2005).
91. N.A. Pertsev, A.G. Zembilgotov, A.K. Tagantsev, *Phys. Rev. Lett.* **80**, 1988 (1998).
92. O. Diéguez, S. Tinte, A. Antons, C. Bungaro, J.B. Neaton, K.M. Rabe, D. Vanderbilt, *Phys. Rev B* **69**, 212101 (2004).
93. Y.L. Li, L.Q. Chen, *Appl. Phys. Lett.* **88**, 072905 (2006).
94. D.A. Tenne, P. Turner, J.D. Schmidt, M. Biegalski, Y.L. Li, L.Q. Chen, A. Soukiassian, S. Trolier-McKinstry, D.G. Schlom, X.X. Xi, D.D. Fong, P.H. Fuoss, J.A. Eastman, G.B. Stephenson, C. Thompson, S.K. Streiffer, *Phys. Rev. Lett.* **103**, 177601 (2009).
95. A. Pertsev, V.G. Koukhar, *Phys. Rev. Lett.* **84**, 3722 (2000).
96. V.G. Koukhar, N.A. Pertsev, R. Waser, *Phys. Rev. B* **64**, 214103 (2001).
97. Y.L. Li, S.Y. Hu, Z.K. Liu, L.Q. Chen, *Appl. Phys. Lett.* **78**, 3878 (2001).
98. Y.L. Li, S.Y. Hu, Z.K. Liu, L.Q. Chen, *Acta Mater.* **50**, 395 (2002).
99. S.K. Streiffer, J.A. Eastman, D.D. Fong, C. Thompson, A. Munkholm, M.V.R. Murty, O. Auciello, G.R. Bai, G.B. Stephenson, *Phys. Rev. Lett.* **89**, 067601 (2002).
100. D.D. Fong, G.B. Stephenson, S.K. Streiffer, J.A. Eastman, O. Auciello, P.H. Fuoss, C. Thompson, *Science* **304**, 1650 (2004).
101. K. Abe, N. Yanase, K. Sano, M. Izuha, N. Fukushima, T. Kawakubo, *Integr. Ferroelectr.* **21**, 197 (1998).
102. N. Yanase, K. Abe, N. Fukushima, T. Kawakubo, *Jpn. J. Appl. Phys., Part 1* **38**, 5305 (1999).
103. E.D. Specht, H.-M. Christen, D.P. Norton, L.A. Boatner, *Phys. Rev. Lett.* **80**, 4317 (1998).
104. H.-M. Christen, L.A. Knauss, K.S. Harshavardhan, *Mater. Sci. Eng., B* **56**, 200 (1998).
105. H.M. Christen, E.D. Specht, S.S. Silliman, K.S. Harshavardhan, *Phys. Rev. B* **68**, 20101 (2003).
106. M. Dawber, C. Lichtensteiger, M. Cantoni, M. Veithen, P. Ghosez, K. Johnston, K.M. Rabe, J.-M. Triscone, *Phys. Rev. Lett.* **95**, 177601 (2005).
107. E. Bousquet, M. Dawber, N. Stucki, C. Lichtensteiger, P. Hermet, S. Gariglio, J.M. Triscone, P. Ghosez, *Nature* **452**, 732 (2008).
108. J.B. Neaton, K.M. Rabe, *Appl. Phys. Lett.* **82**, 1586 (2003).
109. D.A. Tenne, A. Bruchhausen, N.D. Lanzillotti-Kimura, A. Fainstein, R.S. Katiyar, A. Cantarero, A. Soukiassian, V. Vaithyanathan, J.H. Haeni, W. Tian, D.G. Schlom, K.J. Choi, D.M. Kim, C.B. Eom, H.P. Sun, X.Q. Pan, Y.L. Li, L.Q. Chen, Q.X. Jia, S.M. Nakhmanson, K.M. Rabe, X.X. Xi, *Science* **313**, 1614 (2006).
110. Y.L. Li, S.Y. Hu, D. Tenne, A. Soukiassian, D.G. Schlom, X.X. Xi, K.J. Choi, C.B. Eom, A. Saxena, T. Lookman, Q.X. Jia, L.Q. Chen, *Appl. Phys. Lett.* **91**, 112914 (2007).
111. Y.L. Li, S.Y. Hu, D. Tenne, A. Soukiassian, D.G. Schlom, L.Q. Chen, X.X. Xi, K.J. Choi, C.B. Eom, A. Saxena, T. Lookman, Q.X. Jia, *Appl. Phys. Lett.* **91**, 252904 (2007).
112. N. Sai, B. Meyer, D. Vanderbilt, *Phys. Rev. Lett.* **84**, 5636 (2000).
113. M.R. Warusawithana, E.V. Colla, J.N. Eckstein, M.B. Weissman, *Phys. Rev. Lett.* **90**, 036802 (2003).
114. H.N. Lee, H.M. Christen, M.F. Chisholm, C.M. Rouleau, D.H. Lowndes, *Nature* **433**, 395 (2005).
115. A.G. Zembilgotov, N.A. Pertsev, U. Böttger, R. Waser, *Appl. Phys. Lett.* **86**, 052903 (2005).

https://doi.org/10.1557/mrs.2014.1 Published online by Cambridge University Press

116. G. Sheng, Y.L. Li, J.X. Zhang, S. Choudhury, Q.X. Jia, V. Gopalan, D.G. Schlom, Z.K. Liu, L.Q. Chen, *J. Appl. Phys.* **108**, 084113 (2010).
117. K. Kathan-Galipeau, P.P. Wu, Y.L. Li, L.Q. Chen, A. Soukiassian, X.X. Xi, D.G. Schlom, D.A. Bonnell, *ACS Nano* **5**, 640 (2011).
118. K. Kathan-Galipeau, P.P. Wu, Y.L. Li, L.Q. Chen, A. Soukiassian, Y. Zhu, D.A. Muller, X.X. Xi, D.G. Schlom, D.A. Bonnell, *J. Appl. Phys.* **112**, 052011 (2012).
119. J. Ravichandran, A.K. Yadav, R. Cheaito, P.B. Rossen, A. Soukiassian, S.J. Suresha, J.C. Duda, B.M. Foley, C.H. Lee, Y. Zhu, A.W. Lichtenberger, J.E. Moore, D.A. Muller, D.G. Schlom, P.E. Hopkins, A. Majumdar, R. Ramesh, M.A. Zurbuchen, *Nat. Mater.* (2013), in press, doi: 10.1038/nmat3826.
120. J. Wang, J.B. Neaton, H. Zheng, V. Nagarajan, S.B. Ogale, B. Liu, D. Viehland, V. Vaithyanathan, D.G. Schlom, U.V. Waghmare, N.A. Spaldin, K.M. Rabe, M. Wuttig, R. Ramesh, *Science* **299**, 1719 (2003).
121. R. Ramesh, N.A. Spaldin, *Nat. Mater.* **6**, 21 (2007).
122. A.A. Belik, S. Iikubo, K. Kodama, N. Igawa, S.-I. Shamoto, S. Niitaka, M. Azuma, Y. Shimakawa, M. Takano, F. Izumi, E. Takayama-Muromachi, *Chem. Mater.* **18**, 798 (2006).
123. M.-R. Li, U. Adem, S.R.C. McMitchell, Z. Xu, C.I. Thomas, J.E. Warren, D.V. Giap, H. Niu, X. Wan, R.G. Palgrave, F. Schiffmann, F. Cora, B. Slater, T.L. Burnett, M.G. Cain, A.M. Abakumov, G. van Tendeloo, M.F. Thomas, M.J. Rosseinsky, J.B. Claridge, *J. Am. Chem. Soc.* **134**, 3737 (2012).
124. W. Wang, J. Zhao, W. Wang, Z. Gai, N. Balke, M. Chi, H.N. Lee, W. Tian, L. Zhu, X. Cheng, D.J. Keavney, J. Yi, T.Z. Ward, P.C. Snijders, H.M. Christen, W. Wu, J. Shen, X. Xu, *Phys. Rev. Lett.* **110**, 237601 (2013).
125. J.F. Li, J. Wang, M. Wuttig, R. Ramesh, N. Wang, B. Ruette, A.P. Pyatakov, A.K. Zvezdin, D. Viehland, *Appl. Phys. Lett.* **84**, 5261 (2004).
126. R.R. Das, D.M. Kim, S.H. Baek, C.B. Eom, F. Zavaliche, S.Y. Yang, R. Ramesh, Y.B. Chen, X.Q. Pan, X. Ke, M.S. Rzchowski, S.K. Streiffer, *Appl. Phys. Lett.* **88**, 242904 (2006).
127. J. Dho, X. Qi, H. Kim, J.L. MacManus-Driscoll, M.G. Blamire, *Adv. Mater.* **18**, 1445 (2006).
128. F. Kubel, H. Schmid, *Acta Crystallogr., Sect. B: Struct. Sci.* **46**, 698 (1990).
129. A.J. Hatt, N.A. Spaldin, C. Ederer, *Phys. Rev. B* **81**, 054109 (2010).
130. A.G. Christy, *Acta Crystallogr. Sect. B: Struct. Sci.* **51**, 753 (1995).
131. L. Ehm, K. Knorr, L. Peters, S. Rath, W. Depmeier, *J. Alloys Compd.* **429**, 82 (2007).
132. J. Haines, J.M. Léger, O. Schulte, *Phys. Rev. B* **57**, 7551 (1998).
133. J.X. Zhang, B. Xiang, Q. He, J. Seidel, R.J. Zeches, P. Yu, S.Y. Yang, C.H. Wang, Y.H. Chu, L.W. Martin, A.M. Minor, R. Ramesh, *Nat. Nanotechnol.* **6**, 98 (2011).
134. Q. He, Y.H. Chu, J.T. Heron, S.Y. Yang, W.I. Liang, C.Y. Kuo, H.J. Lin, P. Yu, C.W. Liang, R.J. Zeches, W.C. Kuo, J.Y. Juang, C.T. Chen, E. Arenholz, A. Scholl, R. Ramesh, *Nat. Commun.* **2**, 225 (2011).
135. J.C. Yang, Q. He, S.J. Suresha, C.Y. Kuo, C.Y. Peng, R.C. HaisImaier, M.A. Motyka, G. Sheng, C. Adamo, H.J. Lin, Z. Hu, L. Chang, L.H. Tjeng, E. Arenholz, N.J. Podraza, M. Bernhagen, R. Uecker, D.G. Schlom, V. Gopalan, L.Q. Chen, C.T. Chen, R. Ramesh, Y.H. Chu, *Phys. Rev. Lett.* **109**, 247606 (2012).
136. C.J. Fennie, K.M. Rabe, *Phys. Rev. Lett.* **97**, 267602 (2006).
137. J.P. Rivera, H. Schmid, *Ferroelectrics* **36**, 447 (1981).
138. W. von Wartburg, *Phys. Status Solidi A* **21**, 557 (1974).
139. T. Birol, C.J. Fennie, *Phys. Rev. B 88*, **094103** (2013).
140. T.R. McGuire, M.W. Shafer, R.J. Joenk, H.A. Alperin, S.J. Pickart, *J. Appl. Phys.* **37**, 981 (1966).
141. C.-L. Chien, S. DeBenedetti, F. De S. Barros, *Phys. Rev. B* **10** 3913 (1974).
142. T. Katsufuji, H. Takagi, *Phys. Rev. B* **64**, 054415 (2001).
143. H.-H. Wang, A. Fleet, J.D. Brock, D. Dale, Y. Suzuki, *J. Appl. Phys.* **96**, 5324 (2004).
144. K. Kugimiya, K. Fujita, K. Tanaka, K. Hirao, *J. Magn. Magn. Mater.* **310**, 2268 (2007).
145. S.C. Chae, Y.J. Chang, D.-W. Kim, B.W. Lee, I. Choi, C.U. Jung, *J. Electroceram.* **22**, 216 (2009).
146. K. Fujita, N. Wakasugi, S. Murai, Y. Zong, K. Tanaka, *Appl. Phys. Lett.* **94**, 062512 (2009).
147. M.W. Schafer, *J. Appl. Phys.* **36**, 1145 (1965).
148. G.J. McCarthy, W.B. White, R. Roy, *J. Inorg. Nucl. Chem.* **31**, 329 (1969).
149. Y.S. Kim, D.J. Kim, T.H. Kim, T.W. Noh, J.S. Choi, B.H. Park, J.-G. Yoon, *Appl. Phys. Lett.* **91**, 042908 (2007).
150. K.A. Müller, H. Burkard, *Phys. Rev. B* **19**, 3593 (1979).
151. E.J. Tarsa, E.A. Hachfeld, F.T. Quinlan, J.S. Speck, M. Eddy, *Appl. Phys. Lett.* **68**, 490 (1996).
152. T. Ohnishi, M. Lippmaa, T. Yamamoto, S. Meguro, H. Koinuma, *Appl. Phys. Lett.* **87**, 2419191 (2005).
153. T. Ohnishi, K. Shibuya, T. Yamamoto, M. Lippmaa, *J. Appl. Phys.* **103**, 103703 (2008).
154. M. Kestigian, J.G. Dickinson, R. Ward, *J. Am. Chem. Soc.* **79**, 5598 (1957).
155. D.A. Tenne, I.E. Gonenli, A. Soukiassian, D.G. Schlom, S.M. Nakhmanson, K.M. Rabe, X.X. Xi, *Phys. Rev. B* **76**, 024303 (2007).
156. C.M. Brooks, L. Fitting Kourkoutis, T. Heeg, J. Schubert, D.A. Muller, D.G. Schlom, *Appl. Phys. Lett.* **94**, 162905 (2009).
157. J.H. Lee, X. Ke, N.J. Podraza, L. Fitting Kourkoutis, T. Heeg, M. Roeckerath, J.W. Freeland, C.J. Fennie, J. Schubert, D.A. Muller, P. Schiffer, D.G. Schlom, *Appl. Phys. Lett.* **94**, 212509 (2009).
158. J.H. Lee, K.M. Rabe, *Phys. Rev. Lett.* **104**, 207204 (2010).
159. E. Bousquet, N.A. Spaldin, P. Ghosez, *Phys. Rev. Lett.* **104**, 037601 (2010).
160. P.J. Ryan, J.-W. Kim, T. Birol, P. Thompson, J.-H. Lee, X. Ke, P.S. Normile, E. Karapetrova, P. Schiffer, S.D. Brown, C.J. Fennie, D.G. Schlom, *Nat. Commun.* **4**, 1334 (2013).
161. C.H. Lee, N.D. Orloff, T. Birol, Y. Zhu, V. Goian, E. Rocas, R. HaisImaier, E. Vlahos, J.A. Mundy, L.F. Kourkoutis, Y. Nie, M.D. Biegalski, J. Zhang, M. Bernhagen, N.A. Benedek, Y. Kim, J.D. Brock, R. Uecker, X.X. Xi, V. Gopalan, D. Nuzhnyy, S. Kamba, D.A. Muller, I. Takeuchi, J.C. Booth, C.J. Fennie, D.G. Schlom, *Nature* **502**, 532 (2013).
162. O.G. Vendik, *Ferroelectrics* **12**, 85 (1976).
163. S.W. Kirchoefer, J.M. Pond, A.C. Carter, W. Chang, K.K. Agarwal, J.S. Horwitz, D.B. Chrisey, *Microwave Opt. Technol. Lett.* **18**, 168 (1998).
164. S.S. Gevorgian, E.L. Kollberg, *IEEE Trans. Microwave Theory Tech.* **49**, 2117 (2001).
165. A.K. Tagantsev, V.O. Sherman, K.F. Astafiev, J. Venkatesh, N. Setter, *J. Electroceram.* **11**, 5 (2003).
166. S. Andersson, A.D. Wadsley, *Nature* **211**, 581 (1966).
167. J.S Anderson, J.M. Browne, A.K. Cheetham, R. Vondreel, J.L. Hutchison, F.J. Lincoln, D.J.M. Bevan, J. Straehle, *Nature* **243**, 81 (1973).
168. R.J.D. Tilley, *Nature* **269**, 229 (1977).
169. R.J.D. Tilley, *J. Solid State Chem.* **21**, 293 (1977).
170. T. Nakamura, P.H. Sun, Y.J. Shan, Y. Inaguma, M. Itoh, I.S. Kim, J.H. Sohn, M. Ikeda, T. Kitamura, H. Konagaya, *Ferroelectrics* **196**, 205 (1997).
171. P.L. Wise, I.M. Reaney, W.E. Lee, T.J. Price, D.M. Iddles, D.S. Cannell, *J. Eur. Ceram. Soc.* **21**, 1723 (2001).
172. N.D. Orloff, W. Tian, C.J. Fennie, C.H. Lee, D. Gu, J. Mateu, X.X. Xi, K.M. Rabe, D.G. Schlom, I. Takeuchi, J.C. Booth, *Appl. Phys. Lett.* **94**, 042908 (2009).
173. T. Birol, N.A. Benedek, C.J. Fennie, *Phys. Rev. Lett.* **107**, 257602 (2011).
174. D.O. Klenov, W. Donner, B. Foran, S. Stemmer, *Appl. Phys. Lett.* **82**, 3427 (2003).
175. W. Donner, C. Chen, M. Liu, A.J. Jacobson, Y.-L. Lee, M. Gadre, D. Morgan, *Chem. Mater.* **23**, 984 (2011).
176. J.M. Rondinelli, N.A. Spaldin, *Adv. Mater.* **23**, 3363 (2011).
177. J.M. Rondinelli, S.J. May, J.W. Freeland, *MRS Bull.* **37**, 261 (2012).
178. W.S. Choi, J.-H. Kwon, H. Jeen, J.E. Hamann-Borrero, A. Radi, S. Macke, R. Sutarto, F. He, G.A. Sawatzky, V. Hinkov, M. Kim, H.N. Lee, *Nano Lett.* **12**, 4966 (2012).
179. Y. Yang, C.M. Schlepütz, C. Adamo, D.G. Schlom, R. Clarke, *APL Mater.* **1**, 052102 (2013).
180. C.-L. Jia, V. Nagarajan, J.-Q. He, L. Houben, T. Zhao, R. Ramesh, K. Urban, R. Waser, *Nat. Mater.* **6**, 64 (2006).
181. C.-L. Jia, S.-B. Mi, K. Urban, I. Vrejoiu, M. Alexe, D. Hesse, *Nat. Mater.* **7**, 57 (2008).
182. C.T. Nelson, B. Winchester, Y. Zhang, S.-J. Kim, A. Melville, C. Adamo, C.M. Folkman, S.-H. Baek, C.-B. Eom, D.G. Schlom, L.-Q. Chen, X. Pan, *Nano Lett.* **11**, 828 (2011).
183. C.L. Jia, K.W. Urban, M. Alexe, D. Hesse, I. Vrejoiu, *Science* **331**, 1420 (2011).
184. A.Y. Borisevich, H.J. Chang, M. Huijben, M.P. Oxley, S. Okamoto, M.K. Niranjan, J.D. Burton, E.Y. Tsymbal, Y.H. Chu, P. Yu, R. Ramesh, S.V. Kalinin, S.J. Pennycook, *Phys. Rev. Lett.* **105**, 087204 (2010).
185. D.A. Muller, L.F. Kourkoutis, M. Murfitt, J.H. Song, H.Y. Hwang, J. Silcox, N. Dellby, O.L. Krivanek, *Science* **319**, 1073 (2008).
186. D. Lee, R. Behera, P. Wu, H. Xu, Y.L. Li, S.B. Sinnott, S. Phillpot, L. Chen, V. Gopalan, *Phys. Rev. B* **80**, 060102 (2009).
187. E.F. Kneller, R. Hawig, *Magnetics, IEEE Trans. Magn.* **27**, 3588 (1991).
188. E.E. Fullerton, J.S. Jiang, S.D. Bader, *J. Magn. Magn. Mater.* **200**, 392 (1999).
189. P. Wu, X. Ma, Y. Li, V. Gopalan, L.Q. Chen, *Appl. Phys. Lett.* **100**, 092905 (2012).
190. J.H. Lee, K.M. Rabe, *Phys. Rev. Lett.* **107**, 067601 (2011).
191. D.M. Newns, B.G. Elmegreen, X.-H. Liu, G.J. Martyna, *Adv. Mater.* **24**, 3672 (2012).
192. D. Newns, B. Elmegreen, X. Hu Liu, G. Martyna, *J. Appl. Phys.* **111**, 084509 (2012).
193. R.E. Newnham, J.J. Kramer, W.A. Schulze, L.E. Cross, *J. Appl. Phys.* **49**, 6088 (1978).
194. M.J. Harris, S.T. Bramwell, D.F. McMorrow, T. Zeiske, K.W. Godfrey, *Phys. Rev. Lett.* **79**, 2554 (1997).

https://doi.org/10.1557/mrs.2014.1 Published online by Cambridge University Press

195. C. Fennie, K. Rabe, *Phys. Rev. B* **72**, 100103 (2005).
196. T. Choi, Y. Horibe, H.T. Yi, Y.J. Choi, W. Wu, S.W. Cheong, *Nat. Mater.* **9**, 253 (2010).
197. A. Arkenbout, T. Palstra, T. Siegrist, T. Kimura, *Phys. Rev. B* **74**, 184431 (2006).
198. F. Ye, Y. Ren, Q. Huang, J. Fernandez-Baca, P. Dai, J. Lynn, T. Kimura, *Phys. Rev. B* **73**, 220404 (2006).
199. T. Kimura, Y. Sekio, H. Nakamura, T. Siegrist, A.P. Ramirez, *Nat. Mater.* **7**, 291 (2008).
200. Y. Kitagawa, Y. Hiraoka, T. Honda, T. Ishikura, H. Nakamura, T. Kimura, *Nat. Mater.* **9**, 797 (2010).
201. A.A. Bossak, I.E. Graboy, O.Y. Gorbenko, A.R. Kaul, M.S. Kartavtseva, V.L. Svetchnikov, H.W. Zandbergen, *Chem. Mater.* **16**, 1751 (2004).
202. W. Wang, J. Zhao, W. Wang, Z. Gai, N. Balke, M. Chi, H.N. Lee, W. Tian, L. Zhu, X. Cheng, D.J. Keavney, J. Yi, T.Z. Ward, P.C. Snijders, H.M. Christen, W. Wu, J. Shen, X. Xu, *Phys. Rev. Lett.* **110**, 237601 (2013).
203. E.S. Machlin, P. Chaudhari, in *Synthesis and Properties of Metastable Phases*, E.S. Machlin, T.J. Rowland, Eds. (The Metallurgical Society of AIME, Warrendale, 1980), pp. 11–29.
204. C.P. Flynn, *Phys. Rev. Lett.* **57**, 599 (1986).
205. R. Bruinsma, A. Zangwill, *J. Phys. (Paris)* **47**, 2055 (1986).
206. O.Y. Gorbenko, S.V. Samoilenkov, I.E. Graboy, A.R. Kaul, *Chem. Mater.* **14**, 4026 (2002).
207. J.M. Rondinelli, C.J. Fennie, *Adv. Mater.* **24**, 1961 (2012).
208. A.T. Mulder, N.A. Benedek, J.M. Rondinelli, C.J. Fennie, *Adv. Funct. Mater.* **23**, 4810 (2013).
209. C.J. Fennie, *Phys. Rev. Lett.* **100**, 167203 (2008).
210. T. Varga, A. Kumar, E. Vlahos, S. Denev, M. Park, S. Hong, T. Sanehira, Y. Wang, C. Fennie, S. Streiffer, X. Ke, P. Schiffer, V. Gopalan, J. Mitchell, *Phys. Rev. Lett.* **103**, 047601 (2009).
211. G. Singh-Bhalla, C. Bell, J. Ravichandran, W. Siemons, Y. Hikita, S. Salahuddin, A.F. Hebard, H.Y. Hwang, R. Ramesh, *Nat. Phys.* **7**, 80 (2010). □

Career Center

JOB SEEKERS MEET YOUR NEXT EMPLOYER!

We'll show off your talents to the world's most prestigious high-tech firms, universities and laboratories. At the 2014 MRS Spring Meeting Career Center, you can access many interesting job postings, visit recruitment booths and interview with prospective employers. Please bring extra copies of your resume for your own use.

The Career Center is FREE to all MRS members and those registered to attend the 2014 MRS Spring Meeting.

ON-SITE REGISTRATION HOURS
Monday, April 21.....1:00 pm – 4:00 pm
(Candidate Registration Only)

CAREER CENTER HOURS
Tuesday, April 22 .....10:00 am – 5:00 pm
Wednesday, April 23.....10:00 am – 5:00 pm

Register and submit your resume today!
www.mrs.org/spring-2014-career-center



Rigaku
Better measurements. Better confidence. Better world.

www.Rigaku.com/products/xrd/smartlab



Powder Diffraction • Thin Film Diffraction • SAXS • In-Plane Grazing Incidence

Rigaku's SmartLab® is the most versatile diffractometer in the world. You can start using all XRD applications from the very first day because of the unique knowledge-based Guidance control software. The available 9 kW line focus X-ray source provides ultimate power for the most demanding applications. Automatic self-alignment ensures that you always collect the best data possible and beam path selection can be made without touching a multilayer optic.

for Material Scientists

The SmartLab combined with a novel two-dimensional detector enables one to measure a large-area reciprocal space map in minutes rather than days.

Rigaku Corporation and its Global Subsidiaries | www.Rigaku.com | info@Rigaku.com

https://doi.org/10.1557/mrs.2014.1 Published online by Cambridge University Press